NASA
Technical
Paper
2296

March 1984

Formulation of Blade-Flutter Spectral Analyses in Stationary Reference Frame

Anatole P. Kurkov

NASA

NASA
Technical
Paper
2296

1984

Formulation of Blade-Flutter Spectral Analyses in Stationary Reference Frame

Anatole P. Kurkov

Lewis Research Center
Cleveland, Ohio

NASA
National Aeronautics
and Space Administration

**Scientific and Technical
Information Branch**

Summary

Analytic representations are developed for the discrete blade deflection and the continuous tip static pressure fields in a stationary reference frame. Considered are the sampling rates equal to the rotational frequency, equal to the blade passing frequency, and for the pressure, equal to a multiple of the blade passing frequency. For the last two rates the expressions for determining the nodal diameters from the spectra are included. A procedure is presented for transforming the complete unsteady pressure field into a rotating frame of reference. The determination of the true flutter frequency by using two sensors is described. To illustrate their use, the developed procedures are used to interpret selected experimental results.

Introduction

Over the past few years several experimental programs have been completed that used stationary transducers to measure the flutter vibrations of rotor blades. These experiments were conducted on full-scale engines installed in an altitude test facility. Two categories of stationary transducers were used: specially designed optical displacement sensors, and commercially available pressure transducers that could be flushmounted in the engine casing or incorporated in a traversing probe.

The optical blade displacement measurements are described in detail in reference 1. Briefly, this method is based on the measurement of reflected light from the blade tips. The incident light from a light source and the reflected light from the blades are transmitted by means of a fiber optics bundle and a lens system. The resulting instantaneous blade tip positions are recorded on a magnetic tape in the form of a pulse train. In addition, a reference pulse (such as a once-per-revolution signal from the rotor shaft) must be recorded to provide the base relative to which the instantaneous blade positions can be measured. Since pressure measurement using miniature high-response transducers is fairly common, it will not be described in this report.

These measurements are attractive because all blades can be viewed with a single sensor. In contrast, for blade-mounted sensors, the number of sensors must equal the number of blades in order to measure the response of all of the blades. In addition, with stationary sensors the complexities and the limitations associated with the signal transmission from a rotating component are completely avoided. On the other hand, the frequency content of the signals is much higher with these sensors, and the quantitative analyses of these measurements are necessarily more complicated. For the displacement data the high-frequency requirement is necessary in order to be able to reproduce and locate precisely the blade pulses. Similarly, for the pressure data this requirement is necessary in order to be able to reconstruct the steep pressure variation (both, the unsteady and the steady state) when crossing from the pressure to the suction surface of a blade. These requirements were met by recording the signals on frequency-modulated tape at a high speed and later reproducing the signals during digitization at a low speed. Typically, the tape speed reduction ratio was 64 and the resulting effective rate of digitization was of the order of 1 MHz. Subsequent data processing and analyses were performed on a minicomputer equipped with extensive storage peripherals.

Stationary sensors were used to measure displacements and pressures during flutter in several previous works (refs. 2 to 5). Special procedures had to be developed to analyze these data. This report documents the analysis methods developed in the past by using mathematical derivations and presents a new procedure that allows the complete pressure spectrum to be interpreted and the complete unsteady pressure field to be transformed into a rotating frame of reference. The derived analytic expressions are particularly essential for the latter procedure. Since the problem is by nature discrete, because there are a discrete number of blades on the rotor, all of the derivations are performed in the discrete domain. From another point of view, because of this property, the digital spectral analysis methods are ideally suited for analyzing experimental data. During the derivations the only restriction imposed on flutter frequency is that it be less than the blade passing frequency.

The experimental results presented in the report were all obtained for shrouded fan rotors operating at part speed and at high incidence. The inlet pressure and temperature were raised significantly above the atmospheric condition and the relative tip Mach number was in the transonic range.

During the course of preparing the report several improvements in the mathematical derivations were made as a result of discussions with Donald C. Braun of the NASA Lewis Research Center.

Symbols

A	amplitude associated with a blade (real)
a	frequency variable in engine orders (eqs. (18), (59), (90))
B	constant (eq. (3))
C	aerodynamic coefficient
c	blade chord
d	displacement in plane of disk (fig. 7)
E	engine order
$\bar{F}$	defined by eq. (44) (complex)

f pressure amplitude (real)

$\bar{f}$ defined by eq. (43) (complex)

$\bar{G}$ cross-power amplitude (complex)

i imaginary unit

j integer, $\Delta j = j_{\dot{u}} - j_a$, $\delta j = j_T - j_F$

k nodal diameter index

L number of samples per blade passage

l counter relative to blade passage

M moment (eq. (152))

m blade counter, increases opposite to direction of rotation

m_r blade counter, increases in direction of rotation

N number of blades

n denotes harmonics (eq. (43))

P unsteady pressure

ΔP suction-side minus pressure-side differential pressure

Q total number of revolutions

q revolution counter

R radius (fig. 5)

r distance from torsional axis along blade chord (fig. 7)

t time

u frequency variable in E's (eqs. (14) and (49))

V relative velocity

W aerodynamic work (eq. (154))

x distance coordinate (fig. 5)

δx deflection along x (fig. 5)

y distance coordinate (fig. 5)

z argument of the gif function

α physical variable associated with a blade

β defined preceding eq. (155)

Γ defined by eq. (93), (103), (132), or (139)

γ phase angle of $\bar{G}$

$\tilde{\gamma}$ phase angle defined by eq. (129)

ϵ small quantity (eq. (151))

ζ distance from leading edge along blade chord

η distance coordinate (fig. 5)

θ deflection angle (fig. 7)

κ nodal diameter index with range given by eq. (14)

Λ defines limits on n (eq. (43))

λ negative of lower limit on κ (eqs. (63) and (48))

μ integer (eqs. (10) and (37))

ν integer (eq. (36))

ξ distance coordinate (fig. 5)

ρ density

σ interblade phase angle (eq. (1))

Φ angular coordinate in rotating frame; increases in direction opposite to rotation

Φ_r angular coordinate in rotating frame; increases in direction of rotation

φ phase angle of $\bar{\alpha}$ (eq. (7))

χ position of torsional axis as a fraction of chord from leading edge

ψ phase angle

$\tilde{\psi}$ phase angle defined by eq. (41)

ω circular frequency

ω_r rotor angular velocity

Subscripts:

a relates to set a (eq. (17))

$\dot{a}$ subscripted variable is incorrectly associated with set a

F false

f flutter

I imaginary part of complex variable

k relates to k^{th} nodal diameter

l relates to l^{th} point

M relates to moment

n relates to n^{th} harmonic

ΔP relates to differential pressure

s steady state

T true

t total value (sum of steady and unsteady components)

u relates to set u (eq. (17))

$\dot{u}$ subscripted variable is incorrectly associated with set u

δx relates to δx

θ relates to θ

κ relates to κ^{th} nodal diameter

μ relates to μ

0 blade number zero

Special symbols:

$\bar{S}$ S is complex

$\hat{S}$ only real part of complex variable $\bar{S}$ has a meaning

$\bar{S}^*$ complex conjugate of $\bar{S}$

$\bar{\mathrm{S}}$ complex amplitude in real spectrum related to complex amplitude $\bar{S}$ in complex spectrum

S' variable associated with second transducer; corresponds to S of first transducer

ΔS where $S = l, m, \nu$, or Φ; denotes displacement increment of second transducer relative to first

Properties of Stationary Spectra

Blade Sampling in a Stationary Reference Frame

Since flutter is a self-excited vibration, it is generally associated with one of the natural modes of the bladed disk assembly. Usually therefore, the ratio of flutter frequency to rotational frequency (i.e., flutter frequency expressed in engine orders, or E's) is nonintegral. It is because of this property that stationary sensors can be used to detect flutter.

All blades in flutter vibrate at the same frequency with a well-defined phase relationship between blades. In the simplest case the phase angle between the neighboring blades (the interblade phase angle) is constant and the vibratory amplitude around the rotor is uniform. For an N-blade rotor the interblade phase angle σ is restricted to N values given by

$$\sigma = \frac{2\pi k}{N} \qquad k = 0, \ldots, N-1 \tag{1}$$

This relationship follows from the periodicity condition that must be satisfied when completing a full circle around the rotor. The stability of the rotor system strongly depends on the value of σ. This follows from both theoretical analyses and experimental observations. The index k also represents the number of diametral nodes (or nodal diameters) around the rotor or equivalently the number of complete cycles around the rotor at any given time.

In terms of the wave equation, therefore, flutter can be described in a rotating frame of reference by

$$\alpha(k, \Phi_r, t) = A_k \cos(\omega_f t - \Phi_r k + \psi_k) \tag{2}$$

where α represents a physical quantity such as the blade displacement or the pressure on the blade surface; A_k is the amplitude; ω_f is flutter frequency; Φ_r is the angular coordinate, positive in the direction of rotation; and ψ_k is the phase angle corresponding to $\Phi_r = 0$ and time $t = 0$. In this section sampling only at the blade locations will be considered, regardless of whether or not a physical variable is also defined in the space between the blades (i.e., static pressure). Thus, Φ_r can take on values only at locations corresponding to the blade positions, and

$$\Phi_r = \frac{2\pi}{N} m_r + B, \qquad m_r = 1, \ldots, N \tag{3}$$

where m_r is the blade number, increasing in the direction of rotation, and B is a constant. Therefore,

$$\alpha(m_r, t) = A_k \cos\left(\omega_f t - \frac{2\pi}{N} m_r k - kB + \psi_k\right) \tag{4}$$

In general, the blade amplitudes and interblade phase angles are not necessarily uniform around the rotor. This occurs, for example, when the single-blade natural frequencies are not all identical; that is, when the rotor blades are mistuned (ref. 6). Then α is given by a summation of possibly all N waves; that is,

$$\alpha(m_r, t) = \sum_{k=0}^{N-1} A_k \cos\left(\omega_f t - \frac{2\pi}{N} m_r k - kB + \psi_k\right) \tag{5}$$

These waves move with respect to the rotor. To find their speed, equation (4) is differenced (in the discrete domain this operation replaces the differentiation) with respect to time, holding α and therefore the argument of the cosine function fixed. That is,

$$\frac{\Delta}{\Delta t}\left(\omega_f t - \frac{2\pi}{N} m_r k - kB + \psi_k\right) = 0$$

or

$$\frac{2\pi\, \Delta m_r}{N\, \Delta t} = \frac{\omega_f}{k}$$

Thus the angular velocity of the k^{th} wave is inversely proportional to k and is positive in the direction of rotation for $k < N/2$. When $k > N/2$, the wave has the appearance of moving opposite to the direction of rotation. For this reason it is frequently more convenient to let $-N/2 \le k \le N/2 - 1$ for even N, and $-(N-1)/2 \le k \le (N-1)/2$ for odd N; then the sign of k indicates directly the sense of the wave propagation. For $k > 0$, the wave is forward, propagating in the direction of rotation; and for $k < 0$ the wave is backward, propagating opposite to rotor rotation. In the subsequent derivations different limits on k will be selected depending on a particular application. However, in general expressions the original limits on k, $0 \le k \le N-1$, will be retained since then no distinction between even N or odd N is necessary.

In terms of complex exponential notation, equation (5) becomes

$$\hat{\alpha} = \bar{\alpha}_{m_r} e^{i\omega_f t} = \sum_{k=0}^{N-1} \bar{A}_k e^{i(\omega_f t - 2\pi m_r k/N - kB)} \tag{6}$$

where α denotes a vector only the real part of which has a physical meaning and

$$\bar{\alpha}_{m_r} = |\bar{\alpha}_{m_r}|\, e^{i\varphi_{m_r}}, \qquad \bar{A}_k = |\bar{A}_k|\, e^{i\psi_k} = A_k\, e^{i\psi_k} \tag{7}$$

From the point of view of a stationary observer t and m_r are not independent since

$$\omega_r t_\mu = -\Phi_r + q2\pi = -\frac{2\pi}{N} m_r - B + q2\pi$$

$$q = 0, \ldots, Q-1 \quad (8)$$

where ω_r is the rotor angular velocity, q is the revolution counter, μ is an integer, and $t = t_\mu$ is discrete. Let now

$$B = -2\pi, \qquad m = N - m_r, \qquad m = 0, \ldots, N-1$$

then

$$\omega_r t_\mu = \frac{2\pi}{N} m + q2\pi = \frac{2\pi}{N}(m + qN) = \frac{2\pi}{N}\mu \quad (9)$$

where

$$\mu = m + qN \qquad \mu = 0, \ldots, QN-1 \quad (10)$$

The blades are therefore renumbered so that for $t \geq 0$, $m \geq 0$. Thus, in a stationary reference frame

$$\hat{\alpha} = \bar{\alpha}_m e^{i(\omega_f/\omega_r)2\pi\mu/N} = \sum_{k=0}^{N-1} \bar{A}_k e^{i[(\omega_f/\omega_r)(m+qN)+km]2\pi/N}$$

$$= \sum_{k=0}^{N-1} \bar{A}_k e^{i(\omega_f/\omega_r + k)(m+qN)2\pi/N}$$

$$= \sum_{k=0}^{N-1} \bar{A}_k e^{i(\omega_f/\omega_r + k)2\pi\mu/N} \quad (11)$$

where in the second line use was made of the periodicity of the exponential function. Note also that m in α_m could be expressed in terms of μ by using the remainder function

$$m = \mu \bmod N = \mu - N \operatorname{gif}\left(\frac{\mu}{N}\right)$$

where gif(z) is defined as the greatest integer that is less than or equal to z and z is real. (Note that although in this equation μ and N are integers, the mod function is defined in the same way when these two variables are real.)

The real part of the left side of equation (11) represents a physical variable α that is being measured, and the real part of the right side can be viewed as a representation of the output of a digital spectral analyzer. In the last line of equation (11) the term in parentheses in the exponential can be interpreted as frequency in units of rotational frequency and $2\pi/N$ as a sampling interval in radians. This representation was found to be convenient and therefore it will be retained in subsequent derivations.

It follows from equation (11) that for each nodal diameter k there will be a separate frequency line in the spectrum of a stationary sensor. This frequency, expressed in engine orders, is shifted away from flutter frequency by k. Because of this shift it is impossible to determine the true flutter frequency from the spectrum. However, as will be shown later, flutter frequency can be determined by using two stationary sensors mounted at the same axial location but at different circumferential locations. Also, in practice, the frequency can be determined from blade-mounted transducers such as strain gages (which are frequently used with stationary sensors).

Having interpreted equation (11) one can leave out the common terms on the two sides in the first line of the equation. This results in

$$\bar{\alpha}_m = \sum_{k=0}^{N-1} \bar{A}_k e^{i2\pi km/N} \quad (12)$$

Except for the omission of the multiplying factor $1/N$, this expression can be recognized (ref. 7) to be the inverse discrete Fourier transform (DFT^{-1}). Therefore the $\bar{A}_k$'s are given in terms of a DFT as follows

$$\bar{A}_k = \frac{1}{N} \sum_{m=0}^{N-1} \bar{\alpha}_m e^{-i2\pi km/N} \quad (13)$$

where the factor $1/N$ is necessary because it was omitted in equation (12).

Provided that the frequency shift ω_f/ω_r in equation (11) is known, the amplitudes and phases for each mode can be easily determined. The details of this procedure include consideration of frequency aliasing and are presented in the next section along with the interpretation of individual blade spectra that result when m in equation (11) is held fixed during sampling.

Interpretation of Folded Spectra

Since m represents a spatial coordinate, equation (12) can be interpreted to give a spatial distribution of amplitude $|\bar{\alpha}_m|$ and the instantaneous temporal phase φ_m. Because $\bar{\alpha}_m$ is complex, all N coefficients $\bar{A}_k$ are independent. On the other hand, for N blades only N samples per revolution are available. Recalling that the number of samples per revolution is equal to the sampling frequency expressed in units of rotational frequency, from sampling theorem (see ref. 7, e.g.), it follows that the folding frequency is $N/2$. This implies that only $N/2$ coefficients for even N and either $(N+1)/2$ (if $(\omega_f/\omega_r) \bmod 1 < 1/2$) or $(N-1)/2$ (if $(\omega_f/\omega_r) \bmod 1 > 1/2$) for odd N could be determined because the frequency associated with the remaining coefficients will be folded. It is shown later, however, that folded frequencies can be predicted so that except for the cases $(\omega_f/\omega_r) \bmod 1 = 1/2$, or 0, all N coefficients can be

obtained from the spectrum. As already mentioned, ω_f/ω_r is assumed to be known.

To be able to determine coefficients in equation (11) from a spectrum, it is convenient to express this equation in terms of an integer κ and a real variable u_κ, which are defined by

$$\left.\begin{aligned} -\frac{\omega_f}{\omega_r} < \kappa < N - \frac{\omega_f}{\omega_r} \\ u_\kappa = \frac{\omega_f}{\omega_r} + \kappa \qquad 0 < u_\kappa < N \end{aligned}\right\} \tag{14}$$

Equation (11) then becomes

$$\hat{\alpha}(\mu) = \sum_\kappa \bar{A}_{u_\kappa} e^{iu_\kappa 2\pi\mu/N} \qquad 0 < u_\kappa < N \tag{15}$$

The u_κ is used in the subscript of the complex amplitude A instead of a more logical subscript κ, because, to begin with, κ's are unknown and u_κ's are determined first from the spectrum. Since ω_f/ω_r is assumed to be known and κ is an integer, it follows from equation (14) that

$$u_\kappa \bmod 1 = \frac{\omega_f}{\omega_r} \bmod 1 \tag{16}$$

This could be used to identify peaks associated with the set u_κ without the knowledge of κ's. However, because, as already mentioned, the data are undersampled, some frequencies associated with ω_f/ω_r will be folded. In general therefore, the stationary spectrum of a measured variable α can be represented as

$$\hat{\alpha}(\mu) = \sum_\kappa \left(\bar{\alpha}_{u_\kappa} e^{iu_\kappa 2\pi\mu/N} + \bar{\alpha}^*_{a_\kappa} e^{iu_\kappa 2\pi\mu/N} \right) \tag{17}$$

where $\bar{\alpha}$ denotes a complex amplitude and a_κ denotes a folded frequency set distinguishable by the property

$$a_\kappa \bmod 1 = 1 - (\omega_f/\omega_r) \bmod 1 \tag{18}$$

Because there can be at most N complex amplitudes $\bar{\alpha}$ for a given κ, only one (either $\bar{\alpha}_{u_\kappa}$ or $\bar{\alpha}_{a_\kappa}$) can be present in equation (17). The ranges for frequencies associated with $\bar{\alpha}$'s are

$$\left.\begin{aligned} 0 < u_\kappa < \frac{N}{2}, \qquad -\frac{\omega_f}{\omega_r} < \kappa < \frac{N}{2} - \frac{\omega_f}{\omega_r} \\ 0 < a_\kappa < \frac{N}{2}, \qquad \frac{N}{2} - \frac{\omega_f}{\omega_r} < \kappa < N - \frac{\omega_f}{\omega_r} \end{aligned}\right\} \tag{19}$$

Note, however, that in equation (17), u_κ in the exponent has the same range as in equation (15). The frequency a_κ can be expressed in terms of u_κ (of eq. (15)) as

$$a_\kappa = N - u_\kappa = N - \left(\frac{\omega_f}{\omega_r} + \kappa \right) \qquad \frac{N}{2} < u_\kappa < N \tag{20}$$

Note that complex amplitudes associated with folded frequencies, as shown in equation (17), must be conjugated.

Complex amplitudes of equation (15) are given by

$$\left.\begin{aligned} \bar{A}_{u_\kappa} = \bar{\alpha}_{u_\kappa} \qquad 0 < u_\kappa < \frac{N}{2} \\ \bar{A}_{u_\kappa} = \bar{\alpha}^*_{a_\kappa} = \bar{\alpha}^*_{N-u_\kappa} \qquad \frac{N}{2} < u_\kappa < N \end{aligned}\right\} \tag{21}$$

They can be relabeled in terms of κ as follows

$$\bar{A}_\kappa = \bar{A}_{u_\kappa - \omega_f/\omega_r} \tag{22}$$

and in terms of k (eq. (12)) as

$$\left.\begin{aligned} \bar{A}_k^{(k)} = \bar{A}_{\kappa+N}^{(\kappa)} \qquad \kappa < 0 \\ \bar{A}_k^{(k)} = \bar{A}_\kappa^{(\kappa)} \qquad \kappa > 0 \end{aligned}\right\} \tag{23}$$

where the ranges of positive and negative κ's, assuming that $\omega_f/\omega_r < N$, are

$$0 \le \kappa < N - \frac{\omega_f}{\omega_r} \qquad -\frac{\omega_f}{\omega_r} < \kappa < 0 \tag{24}$$

By substituting the relation between κ and k implied by equation (23), it follows that

$$0 \le k < N \qquad \text{or} \qquad 0 \le k \le N-1$$

as assumed in equation (12).

Note that because of equations (16) and (18), when $(\omega_f/\omega_r) \bmod 1 = 1/2$, the two sets of frequencies u_κ and a_κ cannot be separated, and consequently, without additional input the k's (and associated $\bar{A}_k$'s) will remain undetermined. However, this situation, just like the case where ω_f/ω_r happens to be an integer, can be avoided in practice by slightly shifting ω_r from the particular value.

Once all $\bar{A}_k$'s are determined from a stationary spectrum, the inverse DFT (eq. (12)), can be used to obtain $\bar{\alpha}_m$'s.

Note that the limits for the two ranges of κ given by equation (19) are not inclusive. Although these limits sufficed for the preceding derivation, for later reference it is useful to derive the precise limits on κ's.

Using the mod function in equations (19) gives

$$-\left(\frac{\omega_f}{\omega_r}-\frac{\omega_f}{\omega_r}\text{mod }1\right)\leq\kappa_u\leq\left(\frac{N}{2}-\frac{\omega_f}{\omega_r}\right)-\left(\frac{N}{2}-\frac{\omega_f}{\omega_r}\text{mod }1\right) \quad (25)$$

$$\left(\frac{N}{2}-\frac{\omega_f}{\omega_r}\right)-\left(\frac{N}{2}-\frac{\omega_f}{\omega_r}\right)\text{mod }1+1\leq\kappa_a\leq(N-1)-\left(\frac{\omega_f}{\omega_r}-\frac{\omega_f}{\omega_r}\text{mod }1\right) \quad (26)$$

For even N, therefore

$$-\left(\frac{\omega_f}{\omega_r}-\frac{\omega_f}{\omega_r}\text{mod }1\right)\leq\kappa_u\leq\frac{N}{2}-1-\left(\frac{\omega_f}{\omega_r}-\frac{\omega_f}{\omega_r}\text{mod }1\right) \quad (27)$$

$$\frac{N}{2}-\left(\frac{\omega_f}{\omega_r}-\frac{\omega_f}{\omega_r}\text{mod }1\right)\leq\kappa_a\leq(N-1)-\left(\frac{\omega_f}{\omega_r}-\frac{\omega_f}{\omega_r}\text{mod }1\right) \quad (28)$$

For odd N the distinction must be made whether $(\omega_f/\omega_r)\text{mod }1$ is less than or greater than 1/2. Thus for $(\omega_f/\omega_r)\text{mod }1<1/2$

$$-\left(\frac{\omega_f}{\omega_r}-\frac{\omega_f}{\omega_r}\text{mod }1\right)\leq\kappa_u\leq\frac{N-1}{2}-\left(\frac{\omega_f}{\omega_r}-\frac{\omega_f}{\omega_r}\text{mod }1\right) \quad (29)$$

$$\frac{N+1}{2}-\left(\frac{\omega_f}{\omega_r}-\frac{\omega_f}{\omega_r}\text{mod }1\right)\leq\kappa_a\leq(N-1)-\left(\frac{\omega_f}{\omega_r}-\frac{\omega_f}{\omega_r}\text{mod }1\right) \quad (30)$$

and for $(\omega_f/\omega_r)\text{mod }1>1/2$

$$-\left(\frac{\omega_f}{\omega_r}-\frac{\omega_f}{\omega_r}\text{mod }1\right)\leq\kappa_u\leq\frac{N-3}{2}-\left(\frac{\omega_f}{\omega_r}-\frac{\omega_f}{\omega_r}\text{mod }1\right) \quad (31)$$

$$\frac{N-1}{2}-\left(\frac{\omega_f}{\omega_r}-\frac{\omega_f}{\omega_r}\text{mod }1\right)\leq\kappa_a\leq(N-1)-\left(\frac{\omega_f}{\omega_r}-\frac{\omega_f}{\omega_r}\text{mod }1\right) \quad (32)$$

Consider now sampling only one particular blade; that is, m during sampling is considered fixed. (Actually, samples can be collected from all blades as they pass the sensor. However, the samples should later be regrouped into N groups so that any one group will contain samples from one particular blade only.) Then,

$$\hat{\alpha}(m,q)=\bar{A}_m\,e^{i(\omega_f/\omega_r)2\pi q} \qquad q=0,\ldots,Q-1 \quad (33)$$

To avoid aliasing, ω_f/ω_r must be less than 1/2. For a practical range of ω_f and ω_r this case can be ruled out, and therefore a single blade spectrum will always contain aliased flutter frequencies.

If $u=(\omega_f/\omega_r)\text{mod }1<1/2$, the flutter frequency will be folded an even number of times and hence

$$\bar{A}_m=(\bar{\alpha}_u)_m \quad (34)$$

If $u=(\omega_f/\omega_r)\text{mod }1>1/2$ in the spectrum, the aliased frequency a, $a=1-(\omega_f/\omega_r)\text{mod }1$, $0<a<1/2$, will be folded an odd number of times and

$$\bar{A}_m=(\bar{\alpha}_a)^*_m \quad (35)$$

Note that the overall (i.e., N samples per revolution) stationary spectrum is folded only once about $N/2$ engine-order frequency, whereas a single blade spectrum is usually folded several times about 1/2 engine-order frequency. This implies, first, poorer peak separation in the single blade spectrum than in the overall spectrum. Second, because most of the noise in measurement systems falls in the low-frequency range (in this particular case of the order of 1/2 E and below), the signal-to-noise ratio of a single blade spectrum will frequently be below that of the overall spectrum. And third, the overall spectrum essentially gives a modal (i.e., in terms of spatial modes associated with each k) expansion of a physical variable, which is in general of greater interest than the individual blade characteristics described by a single blade spectrum. For these reasons most quantitative analyses will be presented in terms of the overall spectra. (An exception to this would arise, for example, during flutter monitoring, when one blade exhibits particularly large deflections. Its displacement spectrum is then desirable, and it is most expediently obtained by sampling only the particular blade.)

Figures 1 and 2 (ref. 4) illustrate the displacement and differential pressure spectra obtained by sampling N ($N=38$) times per revolution. The differential pressure represents the difference between the suction and the pressure sides of the blade and is nondimensionalized by using the inlet dynamic head. The peaks in these spectra are identified by nodal diameters κ, where the range of κ can be obtained from equation (14) by substituting N and the true flutter frequency $\omega_f/\omega_r=8.45$; that is,

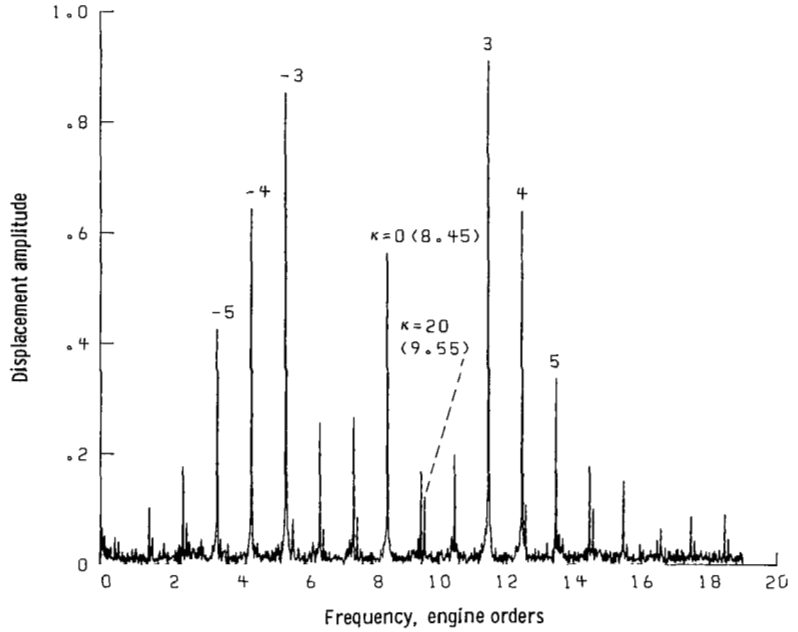

Figure 1. – Displacement amplitude spectrum; port A; 1 unit of displacement $=3.267\times10^{-3}$ radian. Average of four FFT's.

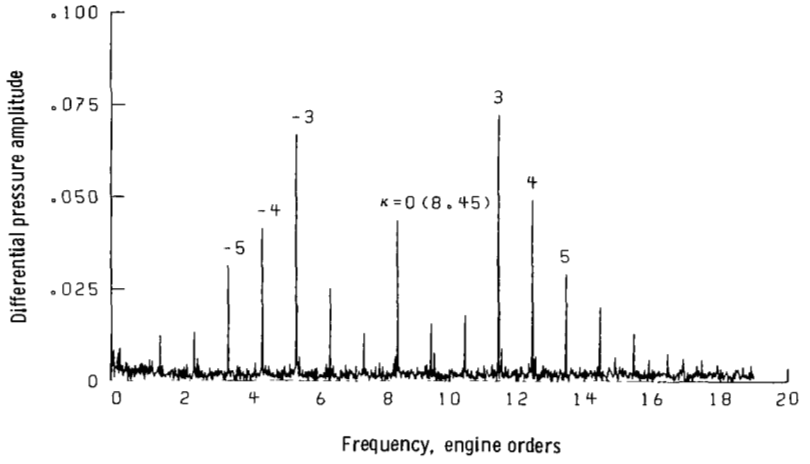

Figure 2. – Differential pressure amplitude spectrum; port 1; amplitude nondimensionalized by using inlet dynamic head. Average of four FFT's.

$-8\leq\kappa\leq29$

Although other less significant nodal diameters associated with $(\omega_f/\omega_r)\bmod 1=0.45$ were not marked in the figures, they can be easily identified by simply counting peaks to the left and right of the zero peak. The most noticeable response associated with $1-(\omega_f/\omega_r)\bmod 1=0.55$ is the peak at $\omega_f/\omega_r=9.55$ (just to the right of the $\kappa=1$ peak at $\omega_f/\omega_r=9.45$). From equation (20) it follows that the corresponding κ for this peak is 20.

One of the essential steps in obtaining a pressure-difference spectrum, such as in figure 2, is determining the blade pressure and suction surface locations. In other words, one needs to establish a criterion by means of which an N-ordered pair of data points representing blade surface pressures can be selected from a continuous stream of data points that encompasses the pressure field for the whole circumference of the rotor. This was accomplished by using the steep pressure gradient region in the steady-state distribution (ref. 3).

Complete Pressure-Field Sampling

In this section a theoretical expression for the complete pressure spectrum will be derived in a form that is most closely related to the measured spectrum obtained by using a fast Fourier transform (FFT) analyzer. Once the interpretation of the measured spectrum (discussed in the next section) is completed, the theoretical expression can always be recast in a more compact form, as shown later.

Since pressure is continuous, the number of samples per revolution is not necessarily limited to the number of blades. Therefore, assume that there are L sampling intervals, $l=0, \ldots, L-1$ per blade passage m, where $m=0, \ldots, N-1$. The spatial dependence of the unsteady pressure can now be described in terms of

$$\nu=l+mL \qquad \nu=0, \ldots, LN-1 \tag{36}$$

However, to describe the time dependence, another variable μ needs to be introduced.

$$\mu=\nu+qLN \qquad \mu=0, \ldots, QLN-1 \tag{37}$$

Note that for $L=1$, μ is consistent with the definition given by equation (10).

Assume that for one particular blade passage ($m=0$), and for a given nodal diameter k, the pressure amplitude distribution is given in terms of the discrete set l by $f_{k,l}$. Similarly, let the discrete temporal phase distribution be given by $\psi_{k,l}$. Then in the rotating frame of reference the pressure field can be expressed as

$$P(k,l,t)=f_{k,l}\cos(\omega_f t+\psi_{k,l})$$

and the instantaneous pressure distribution as

$$P(k,l,0)=f_{k,l}\cos\psi_{k,l}$$

For an arbitrary blade passage m, P becomes

$$P(k,l,m,t)=f_{k,l}\cos\left(\omega_f t+\frac{2\pi km}{N}+\psi_{k,l}\right) \tag{38}$$

(Recall that m increases opposite to the direction of rotation.) In a stationary reference system, in terms of a complex exponential notation, P becomes

$$\hat{P}(k,l,m,\mu)=|\bar{f}_{k,l}|\, e^{i[(\omega_f/\omega_r)2\pi\mu/LN+2\pi km/N+\psi_{k,l}]} \tag{39}$$

where

$$t_\mu=\left(\frac{1}{\omega_r}\right)\left(\frac{2\pi\mu}{LN}\right)$$

Adding and subtracting $2\pi kl/LN$, adding $2\pi kq$ in the exponent, and then using equations (36) and (37) result in

$$\hat{P}(k,l,\mu)=|\bar{f}_{k,l}|\, e^{i[(\omega_f/\omega_r+k)2\pi\mu/LN-2\pi kl/LN+\psi_{k,l}]} \tag{40}$$

Letting

$$\psi_{k,l}=\tilde{\psi}_{k,l}+\frac{2\pi kl}{LN} \tag{41}$$

in equation (40) gives

$$\hat{P}(k,l,\mu)=|\bar{f}_{k,l}|\, e^{i\tilde{\psi}_{k,l}}\, e^{i(\omega_f/\omega_r+k)2\pi\mu/LN} \tag{42}$$

The first term in this equation can be expanded as follows:

$$\bar{f}_{k,l}=|\bar{f}_{k,l}|\, e^{i\tilde{\psi}_{k,l}}=\sum_{n=-\Lambda}^{L-1-\Lambda}\bar{F}_{k,n}\, e^{i2\pi ln/L} \tag{43}$$

where $\Lambda=L/2$ for even L and $\Lambda=(L-1)/2$ for odd L and $\bar{F}_{k,n}$'s are given in terms of a complex DFT by

$$\bar{F}_{k,n}=\frac{1}{L}\sum_{l=0}^{L-1}\bar{f}_{k,l}\, e^{-i2\pi ln/L} \tag{44}$$

If n is restricted to be positive, equation (43) becomes

$$\bar{f}_{k,l}=\sum_{n=1}^{n\le(L-1)/2}\left(\bar{F}_{k,-n}\, e^{-i2\pi ln/L}+\bar{F}_{k,n}\, e^{i2\pi ln/L}\right)$$

$$+\bar{F}_{k,0}+\bar{F}_{k,-L/2}\, e^{-i\pi l} \tag{45}$$

where the upper limit on n is $(L-1)/2$ for odd L and $L/2-1$ for even L, and the last term is included only when L is even. Because the inverse DFT is periodic beyond the sampling interval, μ can be substituted for l in this equation. Performing this substitution and then substituting the resulting expression in equation (42) gives

$$\hat{P}(k,\mu)=\sum_{n=1}^{n\le(L-1)/2}\left(\bar{F}_{k,-n}\, e^{i(\omega_f/\omega_r+k-nN)2\pi\mu/LN}\right.$$

$$\left.+\bar{F}_{k,n}\, e^{i(\omega_f/\omega_r+k+nN)2\pi\mu/LN}\right)+\bar{F}_{k,0}\, e^{i(\omega_f/\omega_r+k)2\pi\mu/LN}$$

$$+\bar{F}_{k,-L/2}\, e^{i(\omega_f/\omega_r+k-LN/2)2\pi\mu/LN} \tag{46}$$

If, in addition, the summation over all possible k is performed, equation (46) becomes

$$\hat{P}(\mu)=\sum_{k=0}^{N-1}\left[\sum_{n=1}^{n\le(L-1)/2}\left(\bar{F}_{k,-n}\, e^{i(\omega_f/\omega_r+k-nN)2\pi\mu/LN}\right.\right.$$

$$\left.+\bar{F}_{k,n}\, e^{i(\omega_f/\omega_r+k+nN)2\pi\mu/LN}\right)+\bar{F}_{k,0}\, e^{i(\omega_f/\omega_r+k)2\pi\mu/LN}$$

$$\left.+\bar{F}_{k,-L/2}\, e^{i(\omega_f/\omega_r+k-LN/2)2\pi\mu/LN}\right] \tag{47}$$

where $2\pi\mu/LN$ is proportional to time. In the next section this equation is used to obtain k's and n's from the measured folded spectrum.

Interpretation of a Complete Pressure Spectrum

To interpret a complete pressure spectrum, it is again convenient to introduce κ instead of k, where as before (eq. (14))

$$-\frac{\omega_f}{\omega_r}<\kappa<N-\frac{\omega_f}{\omega_r}$$

or (48)

$$-\left(\frac{\omega_f}{\omega_r}-\frac{\omega_f}{\omega_r}\bmod 1\right)\leq\kappa\leq N-1-\left(\frac{\omega_f}{\omega_r}-\frac{\omega_f}{\omega_r}\bmod 1\right)$$

Denoting frequency terms by

$$u_{\kappa,\pm n}=\frac{\omega_f}{\omega_r}+\kappa\pm nN \tag{49}$$

equation (47) can be expressed as

$$\hat{P}(\mu)=\sum_{\kappa}\left[\sum_{n=1}^{n\leq(L-1)/2}\left(\bar{F}_{u_{\kappa,-n}}e^{iu_{\kappa,-n}2\pi\mu/LN}+\bar{F}_{u_{\kappa,n}}e^{iu_{\kappa,n}2\pi\mu/LN}\right)+\bar{F}_{u_{k,0}}e^{iu_{\kappa,0}2\pi\mu/LN}+\bar{F}_{u_{\kappa,-L/2}}e^{iu_{\kappa,-L/2}2\pi\mu/LN}\right] \tag{50}$$

The $u_{\kappa,n}$'s in the exponent and in the subscripts of $\bar{F}$'s are used because, to start with, κ's and n's are unknown and these frequencies are the most readily obtained quantities from the measured spectrum. However, once κ's and n's are determined, it is more convenient to denote the complex amplitude as $\bar{F}_{\kappa,n}$.

Because the sampling rate is LN per revolution, folding is expected in the measured spectrum for $u_{\kappa,n}>LN/2$. Therefore for this spectrum equation (50) is replaced by

$$\hat{P}(\mu)=\sum_{\kappa}\left[\sum_{n=1}^{n<(L-1)/2}\left(\bar{\mathfrak{F}}^{*}_{a_{\kappa,n}}e^{iu_{\kappa,-n}2\pi\mu/LN}+\bar{\mathfrak{F}}_{u_{\kappa,n}}e^{iu_{\kappa,n}2\pi\mu/LN}\right)+\bar{\mathfrak{F}}_{u_{\kappa,0}}e^{iu_{\kappa,0}2\pi\mu/LN}+\bar{\mathfrak{F}}^{*}_{a_{\kappa,L/2}}e^{iu_{\kappa,-L/2}2\pi\mu/LN}\right]+\sum_{\kappa<N/2-\omega_f/\omega_r}\bar{\mathfrak{F}}_{u_{\kappa,(L-1)/2}}\times e^{iu_{\kappa,(L-1)/2}2\pi\mu/LN}+\sum_{\kappa>N/2-\omega_f/\omega_r}\bar{\mathfrak{F}}^{*}_{a_{\kappa,(L-1)/2}}e^{iu_{\kappa,(L-1)/2}2\pi\mu/LN} \tag{51}$$

The main purpose of this equation is to define the notation and to illustrate the procedure that follows. That is, it is attempted to associate the aliased $\bar{\mathfrak{F}}$'s with $u_{\kappa,-n}$'s and the unaliased $\bar{\mathfrak{F}}$'s with $u_{\kappa,n}$'s. As proved later, this is correct except for $n=(L-1)/2$, and therefore this term was singled out in equation (51). Note that the ranges for $u_{\kappa,n}$ and $a_{\kappa,n}$ derived below refer to the subscripts of $\bar{\mathfrak{F}}$'s and that $u_{\kappa,\pm n}$'s in the exponents are the same in equations (50) and (51).

First consider the set of frequencies $u_{\kappa,n}$. Substituting the limits on κ from equation (48) into equation (49) gives

$$\left.\begin{aligned}&nN<u_{\kappa,n}<(n+1)N\quad n=0,\ldots,\frac{L-1}{2}\text{ or }\frac{L}{2}-1\\&\text{or}\\&nN+\frac{\omega_f}{\omega_r}\bmod 1\leq u_{\kappa,n}\leq(n+1)N-1+\frac{\omega_f}{\omega_r}\bmod 1\end{aligned}\right\} \tag{52}$$

In addition, the subscript $u_{\kappa,n}$ in equation (51) (but not that in (50)) is restricted by definition to

$$u_{\kappa,n}<\frac{LN}{2}$$

For odd L and $n=(L-1)/2$, it is this condition that limits the subscript $u_{\kappa,n}$ at the upper limit in equation (52). Except for this case, it follows that, by subdividing the measured spectrum into segments given by the inequalities (52), each segment will correspond to consecutive values of n, $n=0,\ldots,L/2-1$ or $(L-3)/2$, and all κ frequencies associated with each n will be contained entirely within each segment n in the order described by inequalities (48). Explicitly, for each n, κ's associated with each $u_{\kappa,n}$ can be determined from

$$\kappa=u_{\kappa,n}-\frac{\omega_f}{\omega_r}-nN \tag{53}$$

where

$$u_{\kappa,n}\bmod 1=\frac{\omega_f}{\omega_r}\bmod 1 \tag{54}$$

is used to identify the peaks that are associated with the u set in the measured spectrum. For odd L, $n=(L-1)/2$, and $u_{\kappa,n}<LN/2$, upon substitution in equation (53),

$$\kappa<\frac{N}{2}-\frac{\omega_f}{\omega_r}$$

For these κ's and n's, the $\bar{F}_{u_{\kappa,n}}$'s (or alternatively $\bar{F}_{\kappa,n}$'s) are given by

$$\bar{F}_{u_{\kappa,n}}=\bar{F}_{\kappa,n}=\bar{\mathfrak{F}}_{u_{\kappa,n}}$$

For the particular case $n=(L-1)/2$ and $\kappa > N/2-\omega_f/\omega_r$, it is shown below that

$$\kappa=(-a_{\kappa,n})-\frac{\omega_f}{\omega_r}+\frac{L+1}{2}N \qquad \frac{L-1}{2}N<a_{\kappa,n}<\frac{LN}{2} \tag{55}$$

where

$$a_{\kappa,n} \bmod 1 = 1-\frac{\omega_f}{\omega_r} \bmod 1 \tag{56}$$

and

$$\bar{F}_{u_{\kappa,n}}=\bar{F}_{\kappa,n}=\bar{\mathfrak{F}}^*_{a_{\kappa,n}} \tag{57}$$

Consider now $u_{\kappa,-n}$ frequencies for which

$$\left.\begin{aligned} &-nN<u_{\kappa,-n}<-(n-1)N \qquad n=1,\ldots,\frac{L}{2} \text{ or } \frac{L-1}{2} \\ &\text{or} \\ &-\left(nN-\frac{\omega_f}{\omega_r} \bmod 1\right) \le u_{\kappa,-n} \le \\ &\qquad -\left[(n-1)N+1-\frac{\omega_f}{\omega_r} \bmod 1\right] \end{aligned}\right\} \tag{58}$$

Since all of these frequencies are negative, they will be associated in the measured spectrum with the set a; that is,

$$u_{\kappa,-n}=-a_{\kappa,n} \tag{59}$$

and

$$\begin{aligned} &(n-1)N<a_{\kappa,n}<nN \qquad n=1,\ldots,\frac{L}{2} \text{ or } \frac{L-1}{2} \\ &\text{or} \\ &(n-1)N+1-\frac{\omega_f}{\omega_r} \bmod 1 \le a_{\kappa,n} \le nN-\frac{\omega_f}{\omega_r} \bmod 1 \end{aligned} \tag{60}$$

These frequencies can be recognized in the spectrum from the property (56). For each value of n.

$$\kappa=(-a_{\kappa,n})-\frac{\omega_f}{\omega_r}+nN \tag{61}$$

and

$$\bar{F}_{u_{\kappa,-n}}=\bar{F}_{\kappa,-n}=\bar{\mathfrak{F}}^*_{a_{\kappa,n}} \tag{62}$$

When L is odd, it follows from equation (60) that for all n's

$$a_{\kappa,n}<\frac{L-1}{2}N$$

Therefore, the range

$$\frac{L-1}{2}N<a_{\kappa,n}<\frac{LN}{2}$$

which is bound by the aliasing condition at the upper end, must be associated with $u_{\kappa,n}$ for $n=(L-1)/2$ and $\kappa > N/2-\omega_f/\omega_r$. (Recall that $u_{\kappa,n}$'s were previously defined only for $\kappa < N/2-\omega_f/\omega_r$ for this n.) Therefore substituting

$$u_{\kappa,n}=LN-a_{\kappa,n} \qquad n=(L-1)/2$$

in equation (53) gives

$$\begin{aligned} \kappa &= LN-a_{\kappa,n}-\frac{\omega_f}{\omega_r}-\frac{L-1}{2}N \\ &= (-a_{\kappa,n})-\frac{\omega_f}{\omega_r}+\frac{L+1}{2}N \end{aligned}$$

which is equation (55). Recognizing the fact that $a_{\kappa,n}$'s are folded frequencies, equations (56) and (57) follow directly.

The particularly interesting case results when $L=1$. Then equation (55) reduces to (20). Thus the results of the section Interpretation of Folded Spectra, obtained for a sampling rate of N per revolution, are recovered.

For practical reasons it is also desirable to express the results in terms of $\bar{F}_{k,n}$'s where $k=0,\ldots,N-1$ and $n_k=0,\ldots,N-1$. The necessary transformation is given for $N-\lambda \le k \le N-1$ and $-\lambda \le \kappa \le -1$ by

$$\bar{F}^{(k)}_{k,n_k}=\bar{F}^{(\kappa)}_{k-N,n_k+1}=\bar{F}^{(\kappa)}_{\kappa,n_\kappa} \begin{cases} 0 \le n_k \le L-2-\Lambda \\ 1 \le n_\kappa \le L-1-\Lambda \end{cases}$$

$$\bar{F}^{(k)}_{k,n_k}=F^{(\kappa)}_{k-N,n_k-L+1}=\bar{F}^{(\kappa)}_{\kappa,-n_\kappa} \begin{cases} L-1-\Lambda \le n_k \le L-2 \\ 1 \le n_\kappa \le \Lambda \end{cases}$$

$$\bar{F}^{(k)}_{k,L-1}=\bar{F}^{(\kappa)}_{k-N,0}=\bar{F}^{(\kappa)}_{\kappa,0} \tag{63a}$$

and for $0 \le k \le N-\lambda-1$ and $0 \le \kappa \le N-1-\lambda$ by

$$\bar{F}^{(k)}_{k,n_k}=\bar{F}^{(\kappa)}_{k,n_k}=\bar{F}^{(\kappa)}_{\kappa,n_\kappa}\quad\begin{cases}0\le n_k\le L-1-\Lambda\\ \\ 0\le n_\kappa\le L-1-\Lambda\end{cases}$$

$$\bar{F}^{(k)}_{k,n_k}=\bar{F}^{(\kappa)}_{k,n_k-L}=F^{(\kappa)}_{\kappa,-n_\kappa}\quad\begin{cases}L-\Lambda\le n_k\le L-1\\ \\ 1\le n_\kappa\le\Lambda\end{cases}\qquad(63b)$$

where $\Lambda=(L-1)/2$ for odd L and $\Lambda=L/2$ for even L and $-\lambda$ denotes the lower limit on κ in equation (48). The k and κ in the superscripts on the F's and in the subscripts on the n's were used to clearly distinguish between the two families of F's and n's. Note that for $L=1$ equations (63) reduce to

$$\bar{F}^{(k)}_{k,0}=\bar{F}^{(\kappa)}_{k-N,0}=\bar{F}^{(\kappa)}_{\kappa,0}\quad N-\lambda\le\kappa\le N-1\qquad-\lambda\le\kappa\le-1$$

$$\bar{F}^{(k)}_{k,0}=\bar{F}^{(\kappa)}_{\kappa,0}\qquad 0\le k\le N-\lambda-1\quad 0\le\kappa\le N-\lambda-1$$

Equations (63) will be derived later.

Thus, all n and k can be determined from the pressure spectrum, again, provided that (ω_f/ω_r) mod 1 is not 1/2 or 0. Note that n for both families, u and a, increases from left to right in the spectrum. However, for aliased frequencies within each n, κ varies from right to left. Since in the spectrum in each n segment there are two different values of n, one associated with set u and the other with set a, to distinguish between the two, one could associate the negative n's with set a. The only exception to this rule arises when L is odd, and $\kappa>N/2-\omega_f/\omega_r$. The aliased frequency in this range is associated with $n=(L-1)/2$. (Negative n's could also be retained in the expressions associated with set a, provided that absolute signs are included with each n.)

Once the $\bar{F}_{k,n}$'s are determined, as shown by equation (43), they can be used as inputs to the complex DFT^{-1} algorithm to obtain $\bar{f}_{k,l}$ for each k. From real and imaginary parts of $\bar{f}_{k,l}$ the distribution of pressure amplitude $|\bar{f}_{k,l}|$ and the instantaneous temporal phase $\psi_{k,l}$ (eq. (41)) can then be obtained for each k. This phase distribution really applies only for blade passage $m=0$. For any other m the entire phase angle in rotating frame of reference (eq. (38)) is

$$\psi_{k,l}+\frac{2\pi km}{N}=\bar{\psi}_{k,l}+\frac{2\pi k(l+mL)}{LN}$$

The instantaneous pressure distribution around the rotor can be obtained as follows

$$\bar{P}(l,m,0)=\sum_{k=0}^{N-1}|\bar{f}_{k,l}|\,e^{i[\bar{\psi}_{k,l}+2\pi k(l+mL)/LN]}\qquad(64)$$

which again involves the use of the inverse DFT. From the real and imaginary parts of $\bar{P}$ the pressure amplitude and the instantaneous temporal phase distributions in a rotating frame of reference can then be constructed.

Equation (64) will now be used as a starting point to prove equations (63). To simplify the derivation, it will be assumed at first that n_k and n_κ have the same range, that is,

$$n_k=0,\ldots,N-1\qquad n_\kappa=0,\ldots,N-1$$

Substituting equation (43) with $\Lambda=0$ into equation (64) gives

$$\bar{P}(l,m,0)=\sum_{k=0}^{N-1}\sum_{n_k=0}^{L-1}\bar{F}^{(k)}_{k,n_k}\,e^{i2\pi ln_k/L}\,e^{i2\pi kl/LN}\,e^{i2\pi km/N}\qquad(65)$$

Since

$$k=\kappa+N\qquad-\Lambda\le\kappa\le-1\qquad N-\lambda\le k\le N-1$$

$$k=\kappa\qquad 0\le\kappa\le N-1-\lambda\qquad 0\le k\le N-1-\lambda$$

only the following part of the summation with respect to k from equation (65) need be examined:

$$\sum_{k=N-\lambda}^{N-1}\sum_{n_k=0}^{L-1}\bar{F}^{(k)}_{k,n_k}\,e^{i2\pi ln_k/L}\,e^{i2\pi kl/LN}\,e^{i2\pi km/N}$$

where $-\lambda$ denotes the lower limit on κ in equation (48). After substituting $k=\kappa+N$ and using the periodicity property of the exponential function, the preceding expression becomes

$$\sum_{\kappa=-\lambda}^{-1}\sum_{n_k=0}^{L-1}\bar{F}^{(k)}_{\kappa+N,n_k}\,e^{i2\pi l(n_k+1)/L}\,e^{i2\pi\kappa l/LN}\,e^{i2\pi\kappa m/N}$$

Now substituting $n_\kappa=n_k+1$ gives

$$\sum_{\kappa=-\lambda}^{-1}\sum_{n_\kappa=1}^{L}\bar{F}^{(k)}_{\kappa+N,n_\kappa-1}\,e^{i2\pi ln_\kappa/L}\,e^{i2\pi\kappa l/LN}\,e^{i2\pi\kappa m/N}$$

$$=\sum_{\kappa=-\lambda}^{-1}\sum_{n_\kappa=0}^{L-1}F^{(\kappa)}_{\kappa,n_\kappa}\,e^{i2\pi ln_\kappa/L}\,e^{i2\pi\kappa l/LN}\,e^{i2\pi\kappa m/N}\qquad(66)$$

The right side of equation (66) corresponds to the part of the summation for negative κ that would be obtained if κ were used instead of k in equation (65). Therefore term-by-term comparison of the two sides of equation (66) gives

$$\left.\begin{aligned} &\bar{F}^{(\kappa)}_{\kappa,n_\kappa}=\bar{F}^{(k)}_{\kappa+N,n_{\kappa-1}}=\bar{F}^{(k)}_{k,n_k} \qquad 1\le n_\kappa\le L-1\\ &\bar{F}^{(\kappa)}_{\kappa,0}=\bar{F}^{(k)}_{\kappa+N,L-1} \end{aligned}\right\} -\lambda\le\kappa\le -1$$

In the remaining range of κ

$$\bar{F}^{(\kappa)}_{\kappa,n_\kappa}=\bar{F}^{(k)}_{k,n_\kappa} \qquad 0\le n_\kappa\le L-1 \qquad 0\le\kappa\le N-\lambda-1$$

These equations can also be expressed in terms of k and n_k as follows

$$\left.\begin{aligned} &\bar{F}^{(k)}_{k,n_k}=\bar{F}^{(\kappa)}_{\kappa-N,n_k+1} \qquad 0\le n_k\le L-2\\ &\bar{F}^{(k)}_{k,L-1}=\bar{F}^{(\kappa)}_{\kappa-N,0} \end{aligned}\right\} N-\lambda\le k\le N-1$$

$$\bar{F}^{(k)}_{k,n_k}=\bar{F}^{(\kappa)}_{\kappa,n_\kappa} \qquad 0\le n_k\le L-1 \qquad 0\le k\le N-\lambda-1 \tag{67}$$

It is now necessary to derive the transformation between the $F^{(n)}_{k,n}$ and $F^{(n_\Lambda)}_{k,n_\Lambda}$, where the range of k must be the same for both F's and

$$0\le n\le L-1 \qquad -\Lambda\le n_\Lambda\le L-1-\Lambda$$

In the derivation, the range of k is assumed to be $k=0, \ldots, N-1$; however, the results do not depend on this choice and any other range could have been selected.

When we use the preceding notation, equation (65) becomes

$$\bar{P}(l,m,0)=\sum_{k=0}^{N-1}\sum_{n=0}^{L-1}\bar{F}^{(n)}_{k,n}\,e^{i2\pi ln/L}\,e^{i2\pi kl/LN}\,e^{i2\pi km/N}$$

The part of the summation for $L-\Lambda\le n\le L-1$ is

$$\sum_{k=0}^{N-1}\sum_{n=L-\Lambda}^{L-1}\bar{F}^{(n)}_{k,n}\,e^{i2\pi ln/L}\,e^{i2\pi kl/LN}\,e^{i2\pi km/N}$$

Substituting $n=n_\Lambda+L$ in the preceding expression and then using periodicity of the exponential function result in

$$\sum_{k=0}^{N-1}\sum_{n_\Lambda=-\Lambda}^{-1}\bar{F}^{(n)}_{k,n_\Lambda+L}\,e^{i2\pi ln_\Lambda/L}\,e^{i2\pi kl/LN}\,e^{i2\pi km/N}$$

$$=\sum_{k=0}^{N-1}\sum_{n_\Lambda=-\Lambda}^{-1}\bar{F}^{(n_\Lambda)}_{k,n_\Lambda}\,e^{i2\pi ln_\Lambda/L}\,e^{i2\pi kl/LN}\,e^{i2\pi km/N}$$

The right side of this equation was obtained from the expression for $\bar{P}(l,m,0)$, written in terms of $F^{(n_\Lambda)}_{k,n_\Lambda}$, by including only the part of the summation corresponding to negative n_Λ. Term-by-term comparison of the two sides of the preceding equation then gives

$$\left.\begin{aligned} &\bar{F}^{(n_\Lambda)}_{k,n_\Lambda}=\bar{F}^{(n)}_{k,n_\Lambda+L}=F^{(n)}_{k,n} \qquad -\Lambda\le n_\Lambda\le -1\\ &\text{or}\\ &\bar{F}^{(n)}_{k,n}=\bar{F}^{(n_\Lambda)}_{k,n-L}=F^{(n_\Lambda)}_{k,n_\Lambda} \qquad L-\Lambda\le n\le L-1\\ &\bar{F}^{(n)}_{k,n}=\bar{F}^{(n_\Lambda)}_{k,n_\Lambda} \qquad 0\le n\le L-\Lambda-1 \end{aligned}\right\} \tag{68}$$

where the last equation was added to complete the range on n.

Equations (63) result by consecutive application of equations (67) and (68) with an additional slight modification resulting from the restriction that n be positive. Thus the negative sign must be carried into the second subscript of F.

Figure 3 illustrates the complete unsteady pressure spectrum for the same flutter point as for the spectra in figures 1 and 2. Hence $\omega_f/\omega_r=8.45$ and $N=38$. For the set u frequencies

$$\frac{\omega_f}{\omega_r}\bmod 1=0.45$$

which identifies the associated peaks in the spectrum. The spectrum can now be subdivided into segments each $38E$ long. For the frequency set u, the first segment corresponds to $n=0$ and the last (which is only partly included) to $n=6$. Equation (53) is now used to determine κ associated with each u frequency marked in the particular n segment. The resulting κ's and n's were also marked in the figure.

For the set a

$$1-\frac{\omega_f}{\omega_r}\bmod 1=0.55$$

and the $38E$ segments in the figure were numbered beginning with $n=1$ and ending with $n=7$ (which is incomplete). Equation (61) was then used to determine κ's associated with each a frequency marked in the particular n segment. Once κ's were determined for this set, they were negated to distinguish them from positive n's associated with the set u. The resulting κ's and n's were then marked in the figure. (Note that one can introduce negative n's with this set of frequencies from the start provided that n is replaced with $|n|$ in eq. (61).)

Another example of a complete pressure-field spectrum obtained for an earlier build of this fan rotor

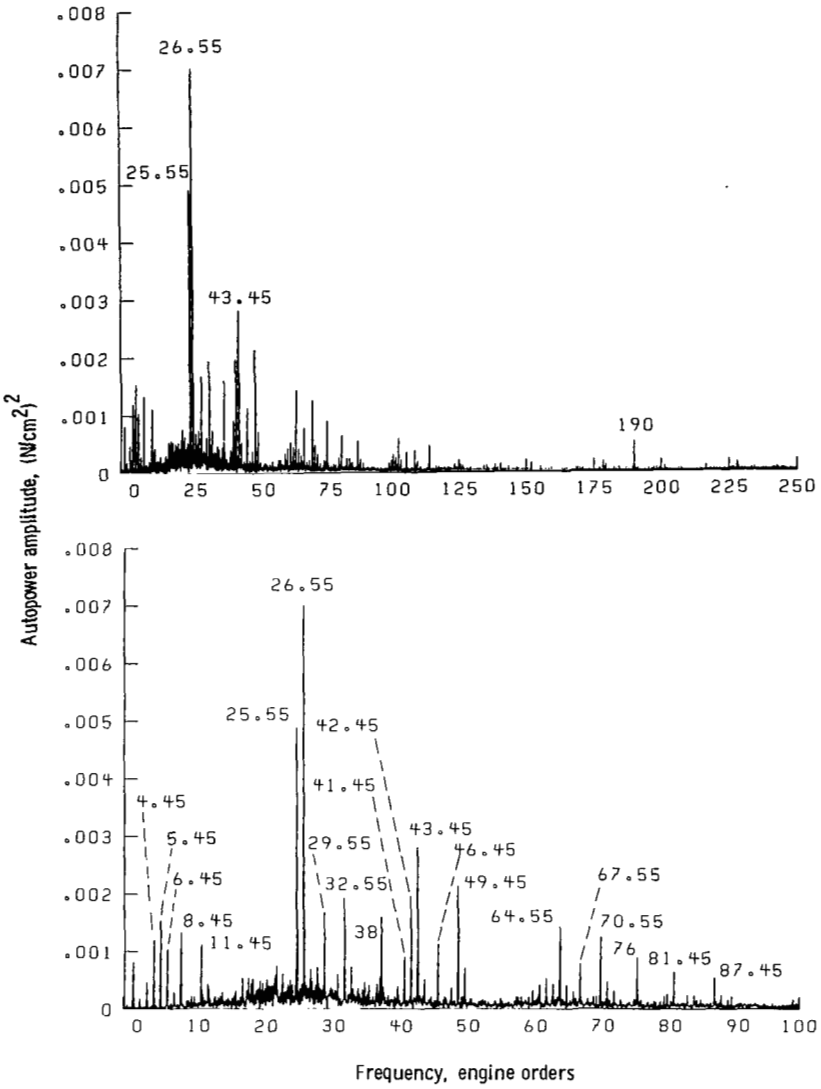

n=0		n=-1		n=1		n=-2		n=2	
FRQ.(E)	κ	FRQ.(E)	κ	FRQ.(E)	κ	FRQ.(E)	κ	FRQ.(E)	κ
4.45	-4	25.55	4	41.45	-5	64.55	3	81.45	-3
5.45	-3	26.55	3	42.45	-4	67.55	0	87.45	3
6.45	-2	29.55	0	43.45	-3	70.55	-3		
8.45	0	32.55	-3	49.45	3				
11.45	3								

(a) To 250 engine orders.
(b) Zero to 100-engine-order portion of spectrum in fig. 3(a).

Figure 3. – Power spectrum of leading-edge pressure transducer signal; engine A.

(engine B) is given in figure 4. For this figure, $\omega_f/\omega_r = 7.19$ and as before $N = 38$. The response at $\omega/\omega_r = 205.75$ is not associated with flutter.

Note that in figures 3 and 4 only the low-order positive and negative κ's and n's are present; this justifies the particular choice of limits on κ and n. In terms of these κ's and n's, equation (47) reduces to

$$\hat{P}(\mu) = \sum_{\kappa=-\lambda}^{N-1-\lambda} \sum_{n=-\Lambda}^{L-1-\Lambda} \bar{F}_{\kappa,n}\, e^{j(\omega_f/\omega_r + \kappa + nN)2\pi\mu/LN}$$

where $-\lambda$ denotes the lower limit on κ given by equation (48) and Λ is defined as in equation (43).

In these examples the total number of samples was $QLN = 8192$. Conveniently this number is a power of 2 so

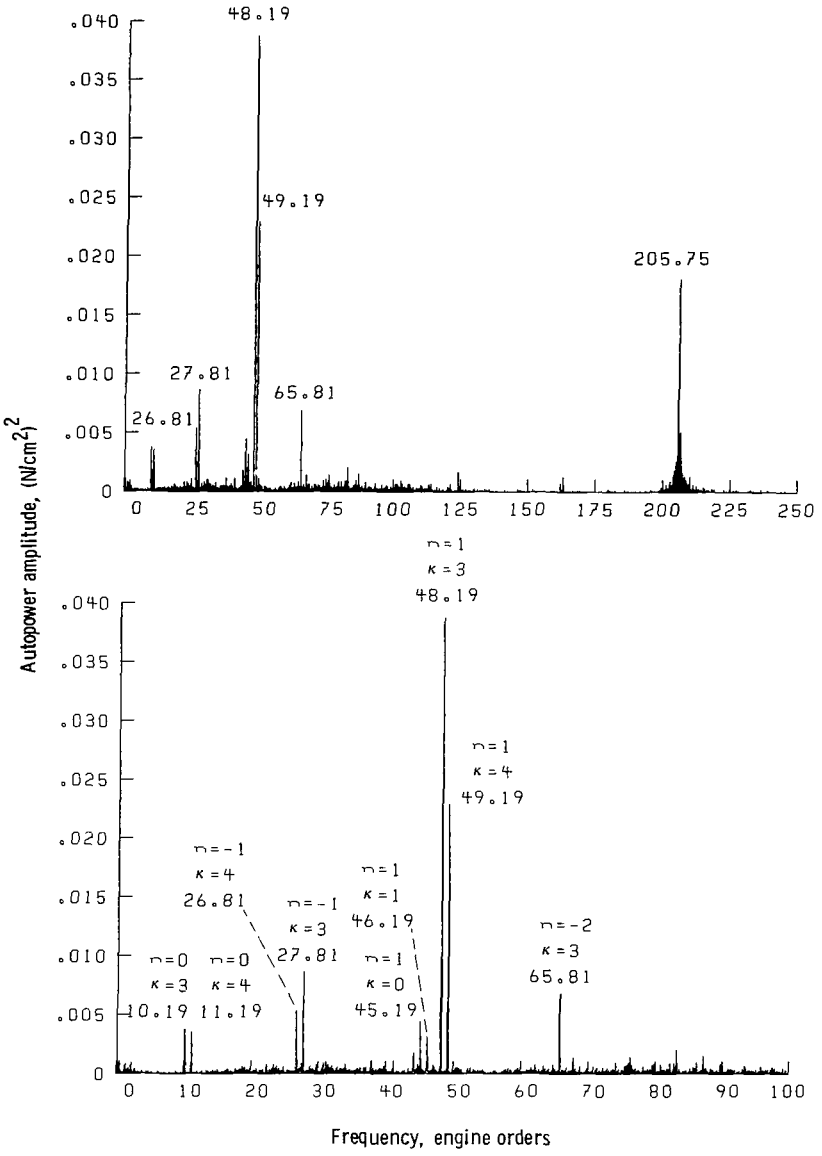

(a) To 250 engine orders.
(b) Zero to 100-engine-order portion of spectrum in fig. 4(a).

Figure 4. – Power spectrum of leading-edge pressure transducer signal; engine B.

that the standard DFT algorithm could be used. Because the number of revolutions Q was 16, the sampling rate LN was 512. Note, however, that for $N=38$ this results in a nonintegral value of L (or more precisely an average L). Strictly speaking the preceding formulas apply only when L is an integer. However, note that L enters the formulas through the product term LN, which also determines the folding sampling rate, and either the $L/2$ or $(L-1)/2$ term in the summation over index n. In the examples, the sampling rate selected was sufficiently high so that the terms associated with the tail end of the spectrum were negligible and hence no difficulties were encountered. This will also be the most frequent case in practice.

It likewise does not seem to be important that Q be an integer. If so desired, however, both Q and L can always be chosen to be integers by using Singleton's algorithm (ref. 8).

Another practical consideration is the fact that in general ω_f/ω_r will not coincide with any frequency line (i.e., will not be a bin-centered case). To evaluate the complex coefficients from the spectrum, it is then best to use the interpolation formulas that were originally derived by Donald C. Braun of Lewis. For completeness these formulas are included in the appendix.

Determination of Flutter Frequency

The true flutter frequency can be determined from a cross-power spectrum between two pressure or two displacement transducers that are located at different circumferential positions. The transducers must, however, correspond to the same axial position.

To examine the spectral relationship between two transducers, an expression analogous to equation (46) or (50) but for an arbitrary spatial reference point is needed. By using this expression, an equation can be derived for the complex cross-power amplitude. From the cross-power phase angle and the known angular separation between the two transducers then, the particular nodal diameter (provided that the sampling rate is at least N) and flutter frequency can be found. Only one complex amplitude is needed from the measured cross-power spectrum. Therefore it is best to choose the maximum amplitude. As will be seen, the angular separation between the transducers can be selected to optimize the determination of frequency.

Consider first the complete pressure-field spectrum. The original spatial reference in the rotating frame, $m=0$ and $l=0$ at $t=0$, will be retained for the first transducer. For the second transducer it will be assumed that, at $t=0$, $m=\Delta m$ and $l=\Delta l$ in the rotating frame of reference. For this transducer it is convenient therefore to introduce the following set of variables:

$$\left.\begin{array}{ll} m'=m-\Delta m & m'=0,\ \ldots,\ N-1;\\ & 0\le\Delta m\le N-1\\ l'=l-\Delta l & l'=0,\ \ldots,\ L-1;\\ & 0\le\Delta l\le L-1\\ \nu'=\nu-\Delta\nu & \nu'=0,\ \ldots,\ LN-1;\\ & 0\le\Delta\nu\le LN-1 \end{array}\right\} \tag{69}$$

which vanish at $t=0$, just like the corresponding unprimed variables for the first transducer.

Equation (38), written for the rotating frame of reference, can be expressed as

$$\hat{P}(k,l,m,t)=|\bar{f}_{k,l}|\ e^{i\psi_{k,l}}\ e^{i(\omega_f t+2\pi km/N)} \tag{70}$$

by using the complex exponential notation. Introducing equations (41), (43), and (36) into this equation results in

$$\hat{P}(k,l,\nu,t)=e^{i(\omega_f t+2\pi k\nu/LN)}\sum_{n=-\Lambda}^{L-1-\Lambda}\bar{F}_{k,n}\ e^{i2\pi ln/L} \tag{71}$$

Substituting now

$$l=(l'+\Delta l)\ \text{mod}\ L$$

$$\nu=(\nu'+\Delta\nu)\ \text{mod}(LN)$$

in equation (71) results in

$$\hat{P}(k,l',\nu',t)=e^{i(\omega_f t+2\pi k\nu'/LN)}\ e^{i2\pi k\Delta\nu/LN}\times\sum_{n=-\Lambda}^{L-1-\Lambda}\bar{F}_{k,n}\ e^{i2\pi n\Delta l/L}\ e^{i2\pi nl'/L} \tag{72}$$

Equation (72) can now be transformed into a stationary reference frame by using

$$t=t_{\mu'}=\frac{1}{\omega_r}\frac{2\pi\mu'}{LN}\qquad \mu'=\nu'+qLN$$

so that

$$\hat{P}(k,l',\nu',\mu')=e^{i[(\omega_f/\omega_r)\mu'+k\nu']2\pi/LN}\ e^{i2\pi k\Delta\nu/LN}\times\sum_{n=-\Lambda}^{L-1-\Lambda}\bar{F}_{k,n}\ e^{i2\pi n\Delta l}\ e^{i2\pi nl'/L}$$

$$=e^{i(\omega_f/\omega_r+k)2\pi\mu'/LN}\ e^{i2\pi k\Delta\nu/LN}\times\sum_{n=-\Lambda}^{L-1-\Lambda}\bar{F}_{k,n}\ e^{i2\pi n\Delta l}\ e^{i2\pi nl'/L} \tag{73}$$

(Note that both $t_{\mu'}$ and t_{μ} equal zero when t is zero.) Since

$$e^{i2\pi nl'/L}=e^{i2\pi n(l'+m'L+q'NL)/L}=e^{i2\pi n\mu'/L}$$

equation (73) can be expressed as

$$\hat{P}(k,\mu')=e^{i2\pi k\Delta\nu/LN}\sum_{n=-\Lambda}^{L-1-\Lambda}\bar{F}_{k,n}\ e^{i2\pi n\Delta l/L}\times e^{i(\omega_f/\omega_r+k+nN)2\pi\mu'/LN} \tag{74}$$

Summing now over k results in

$$\hat{P}(\mu')=\sum_{k=0}^{N-1}e^{i2\pi k\Delta\nu/LN}\sum_{n=-\Lambda}^{L-1-\Lambda}\bar{F}_{k,n}\ e^{i2\pi n\Delta l/L}\times e^{i(\omega_f/\omega_r+k+nN)2\pi\mu'/LN} \tag{75}$$

Note that the expression for the first transducer can be recovered from equation (75) by setting $\Delta l=0$, and $\Delta\nu=0$.

If n is restricted to positive values and if κ (eq. (48)) and $u_{\kappa,n}$ (eq. (49)) are introduced in equation (75), it becomes

$$\hat{P}(\mu') = \sum_{\kappa} e^{i2\pi\kappa\Delta\nu/LN}\left[\sum_{n=1}^{n\le(L-1)/2}\left(\bar{F}_{u_{\kappa,-n}}\, e^{-i2\pi n\Delta l/L} \times e^{iu_{\kappa,-n}2\pi\mu'/LN} + \bar{F}_{u_{\kappa,n}}\, e^{i2\pi n\Delta l/L}\, e^{iu_{\kappa,n}2\pi\mu'/LN}\right) + \bar{F}_{u_{\kappa,0}}\, e^{iu_{\kappa,0}2\pi\mu'/LN} + \bar{F}_{u_{\kappa,-L/2}}\, e^{-i\pi\Delta l}\, e^{iu_{\kappa,-L/2}2\pi\mu'/LN}\right]$$

$$= \sum_{\kappa}\left[\sum_{n=1}^{n\le(L-1)/2}\left(\bar{F}'_{u_{\kappa,-n}}\, e^{iu_{\kappa,-n}2\pi\mu'/LN} + \bar{F}'_{u_{\kappa,n}}\, e^{iu_{\kappa,n}2\pi\mu'/LN}\right) + \bar{F}'_{u_{\kappa,0}}\, e^{iu_{\kappa,0}2\pi\mu'/LN} + \bar{F}'_{u_{\kappa,-L/2}}\, e^{iu_{\kappa,-L/2}2\pi\mu'/LN}\right] \quad (76)$$

In this equation primes denote the complex amplitudes for the second transducer.

The complex cross-power amplitude between the first and second transducer can therefore be expressed as

$$\begin{aligned}\bar{G}_{\kappa,\pm n} &= |\bar{G}_{\kappa,\pm n}|\, e^{i\gamma_{\kappa,\pm n}} = \left(\bar{F}'_{\kappa,\pm n}\right)\left(\bar{F}_{\kappa,\pm n}\right)^* \\ &= \left(\bar{F}_{\kappa,\pm n}\, e^{i2\pi\kappa\Delta\nu/LN}\, e^{\pm i2\pi n\Delta l/L}\right)\left(\bar{F}_{\kappa,\pm n}\right)^* \\ &= |\bar{F}_{\kappa,\pm n}|^2\, e^{i2\pi(\kappa\Delta\nu/LN \pm n\Delta l/L)} \end{aligned} \quad (77)$$

where use was made of the relationship between $\bar{F}'$ and $\bar{F}$ implied by equation (76). Hence

$$\gamma_{\kappa,\pm n} + 2\pi j_{\kappa,\pm n} = 2\pi\left(\frac{\kappa\Delta\nu}{LN} \pm \frac{n\Delta l}{L}\right) \qquad 0 \le \gamma_{\kappa,\pm n} < 2\pi \quad (78)$$

and

$$\kappa = \frac{LN}{\Delta\nu}\left(\frac{\gamma_{\kappa,\pm n}}{2\pi} + j_{\kappa,\pm n}\right) \mp nN\frac{\Delta l}{\Delta\nu} \quad (79)$$

In principle, therefore, one can select some large peak in the complex cross-power spectrum, obtain $\gamma_{\kappa,\pm n}$, solve for κ from equation (79), and then determine ω_f/ω_r from equation (49) by using known κ. In reality, however, because there are two sets of frequencies, *u* and *a*, in the measured spectrum, first a criterion must be developed that will permit one to differentiate between the two sets of frequencies. This is necessary because, as shown below, a different set of equations is associated with set *a*.

Script letters will again be used to denote the complex amplitudes in the real spectrum to distinguish them from the corresponding amplitudes in the complex spectrum. Thus the cross power from the real spectrum for the set *a* is defined by

$$\begin{aligned}\bar{\mathcal{G}}_{a_{\kappa,n}} &= \left(\bar{\mathcal{F}}'_{a_{\kappa,n}}\right)\left(\bar{\mathcal{F}}_{a_{\kappa,n}}\right)^* = \left(\bar{F}'^{*}_{u_{\kappa,-n}}\right)\left(\bar{F}^{*}_{u_{\kappa,-n}}\right)^* \\ &= \left(\bar{F}'_{u_{\kappa,-n}}\right)^*\left(\bar{F}_{u_{\kappa,-n}}\right) \\ &= |\bar{F}_{u_{\kappa,-n}}|^2\, e^{-i2\pi(\kappa_a\Delta\nu/LN - n_a\Delta l/L)} \\ &= \bar{G}^*_{u_{\kappa,-n}} = |\bar{G}_{u_{\kappa,-n}}|\, e^{-i\gamma_{u_{\kappa,-n}}} = |\bar{\mathcal{G}}_{a_{\kappa,n}}|\, e^{i\gamma_{a_{\kappa,n}}} \end{aligned} \quad (80)$$

where again use was made of the relationship between $\bar{F}'$ and $\bar{F}$ implied by equation (76). Therefore

$$\gamma_{a_{\kappa,n}} + 2\pi j_{a_{\kappa,n}} = -2\pi\left(\kappa_a\frac{\Delta\nu}{LN} - n_a\frac{\Delta l}{L}\right) \quad (81)$$

and

$$\kappa_a = -\frac{LN}{\Delta\nu}\left(\frac{\gamma_{a_{\kappa,n}}}{2\pi} + j_{a_{\kappa,n}}\right) + n_a N\frac{\Delta l}{\Delta\nu} \quad (82)$$

where the integer $j_{a_{\kappa,n}}$ depends on κ and n for a selected Δl and $\Delta\nu$. For set *u*, $\bar{F}_{u_{\kappa,n}} = \bar{\mathcal{F}}_{u_{\kappa,n}}$ and from equation (78) it follows, except for $n = (L-1)/2$, odd L, that

$$\kappa_u = \frac{LN}{\Delta\nu}\left(\frac{\gamma_{u_{\kappa,n}}}{2\pi} + j_{u_{\kappa,n}}\right) - n_u N\frac{\Delta l}{\Delta\nu} \quad (83)$$

Since it is not known in advance whether the selected amplitude is associated with the set *u* or the set *a*, it is possible to associate it with the set *u* when in fact it is associated with the set *a*. For this particular case, subscript $\dot{u}$ will be used, with the dot indicating that the complex amplitude was incorrectly assigned to the set *u*. Thus, integer $n_{\dot{u}}$ will be determined from the spectrum according to the rules formulated for the set *u* (in the section Interpretation of a Complete Pressure Spectrum), and subsequently κ will be determined from equation (83). Hence

$$\kappa_{\dot{u}} = \frac{LN}{\Delta\nu}\left(\frac{\gamma_{\dot{u}_{\kappa,n}}}{2\pi} + j_{\dot{u}_{\kappa,n}}\right) - n_{\dot{u}} N\frac{\Delta l}{\Delta\nu} \quad (84)$$

where integer $j_{\dot{u}_{\kappa,n}}$ depends on κ and $n_{\dot{u}}$ for a given Δl and $\Delta\nu$. In turn, ω_f/ω_r depends on $\kappa_{\dot{u}}$ (eq. (53)); that is,

$$\left(\frac{\omega_f}{\omega_r}\right)_{\dot{u}} = \dot{u}_{\kappa,n} - \kappa_{\dot{u}} - n_{\dot{u}} N \quad (85)$$

Thus, in general (whether for frequency set *u*, $\dot{u}$, or *a*) one must first guess the value of j to determine κ and ω_f/ω_r. The resulting κ must be an integer and the resulting ω_f/ω_r must be in the range

$$0<\frac{\omega_f}{\omega_r}<N \tag{86}$$

Thus j and κ will have to be determined iteratively. However, in the case of an incorrect frequency assignment to the set u (i.e., eqs. (84) and (85)), it may not be possible to determine physically plausible values for κ and ω_f/ω_r.

Because by assumption the set a is the correct one, there must be at least one set of values for κ_a, $j_{a_{\kappa,n}}$, and $(\omega_f/\omega_r)_a$ such that the first two are integers and the third one satisfies equation (86). Since $\gamma_{\dot{u}_{\kappa,n}}$ and $\gamma_{a_{\kappa,n}}$ are associated with the same complex amplitude

$$\gamma_{\dot{u}_{\kappa,n}}=\gamma_{a_{\kappa,n}}$$

Using then equations (82) and (84) and $n_a=n_{\dot{u}}+1$ in the above it follows that

$$\frac{\Delta\nu}{LN}\kappa_{\dot{u}}+\frac{n_{\dot{u}}\Delta l}{L}-j_{\dot{u}_{\kappa,n}}=-\frac{\Delta\nu}{LN}\kappa_a+(n_{\dot{u}}+1)\frac{\Delta l}{L}-j_{a_{\kappa,n}}$$

and

$$\kappa_{\dot{u}}=N\frac{\Delta l}{\Delta\nu}-\kappa_a+\frac{LN}{\Delta\nu}\left(j_{\dot{u}_{\kappa,n}}-j_{a_{\kappa,n}}\right) \tag{87}$$

Denoting

$$\Delta j_{\kappa,n}=j_{\dot{u}_{\kappa,n}}-j_{a_{\kappa,n}} \tag{88}$$

equation (87) can be expressed as

$$\kappa_{\dot{u}}=-\kappa_a+N\frac{\Delta j_{\kappa,n}+\Delta l/L}{\Delta m+\Delta l/L} \tag{89}$$

Note that it is only necessary to consider $\Delta m>0$ and $\Delta l>0$ since this can always be achieved by a particular choice of the transducer labeling. (This will also be assumed in all subsequent equations.)

On the other hand, because $\dot{u}_{\kappa,n}=a_{\kappa,n}$, using equation (85) and the following analogous equation for the set a (eq. (61))

$$\left(\frac{\omega_f}{\omega_r}\right)_a=(-a_{\kappa,n})-\kappa_a+n_aN \tag{90}$$

results in

$$\left(\frac{\omega_f}{\omega_r}\right)_{\dot{u}}+\kappa_{\dot{u}}+n_{\dot{u}}N=-\left(\frac{\omega_f}{\omega_r}\right)_a-\kappa_a+n_aN$$

and

$$\left(\frac{\omega_f}{\omega_r}\right)_{\dot{u}}=N-(\kappa_{\dot{u}}+\kappa_a)-\left(\frac{\omega_f}{\omega_r}\right)_a \tag{91}$$

Substituting of $\kappa_{\dot{u}}$ from equation (89) in equation (91) then yields

$$\left(\frac{\omega_f}{\omega_r}\right)_{\dot{u}}=N-\left(\frac{\omega_f}{\omega_r}\right)_a-N\frac{\Delta j_{\kappa,n}+\Delta l/L}{\Delta m+\Delta l/L} \tag{92}$$

Let now

$$\Gamma=N\frac{\Delta j_{\kappa,n}+\Delta l/L}{\Delta m+\Delta l/L} \tag{93}$$

With this definition, applying the mod function to the left and right sides of equation (92) gives

$$\left(\frac{\omega_f}{\omega_r}\right)_{\dot{u}}\bmod 1=\left\{\left[N-\left(\frac{\omega_f}{\omega_r}\right)_a\right]-\Gamma\right\}\bmod 1$$

$$=\left\{\left[N-\left(\frac{\omega_f}{\omega_r}\right)_a\right]\bmod 1-\Gamma\bmod 1\right\}\times\bmod 1$$

$$=\left\{\left[1-\left(\frac{\omega_f}{\omega_r}\right)_a\bmod 1\right]-\Gamma\bmod 1\right\}\times\bmod 1$$

Then, if

$$\Gamma\bmod 1<1-\left(\frac{\omega_f}{\omega_r}\right)_a\bmod 1$$

$$\left(\frac{\omega_f}{\omega_r}\right)_{\dot{u}}\bmod 1=1-\left(\frac{\omega_f}{\omega_r}\right)_a\bmod 1-\Gamma\bmod 1 \tag{94}$$

and if

$$\Gamma\bmod 1>1-\left(\frac{\omega_f}{\omega_r}\right)_a\bmod 1$$

$$\left(\frac{\omega_f}{\omega_r}\right)_{\dot{u}}\bmod 1=1-\left\{\Gamma\bmod 1-\left[1-\left(\frac{\omega_f}{\omega_r}\right)_a\bmod 1\right]\right\}$$

$$=2-\left(\frac{\omega_f}{\omega_r}\right)_a\bmod 1-\Gamma\bmod 1 \tag{95}$$

If $\Gamma\bmod 1=0$, referring to equations (89) and (93) it follows that $\kappa_{\dot{u}}$ will be an integer; that is,

$$\kappa_{\dot{u}}\bmod 1=0$$

However, then from equation (94)

$$\left(\frac{\omega_f}{\omega_r}\right)_{\dot{u}} \bmod 1 = 1 - \left(\frac{\omega_f}{\omega_r}\right)_{a} \bmod 1 \tag{96}$$

Thus if it was assumed incorrectly that the selected peak in the spectrum is associated with the set u, equation (96) will not contradict this assumption. It is therefore necessary that

$$\Gamma \bmod 1 \neq 0$$

Equation (89) then yields

$$\kappa_{\dot{u}} \bmod 1 \neq 0$$

Note also that if $\Gamma \bmod 1 \neq 0$, in general the original value of $(\omega_f/\omega_r)_{\dot{u}} \bmod 1$ will also be changed. The only exceptions are when

$$\Gamma \bmod 1 = 1 - 2\left[\left(\frac{\omega_f}{\omega_r}\right)_{a} \bmod 1\right] \qquad \left(\frac{\omega_f}{\omega_r}\right)_{a} \bmod 1 < \frac{1}{2} \tag{97}$$

in equation (94), and when

$$\Gamma \bmod 1 = 2\left[1 - \left(\frac{\omega_f}{\omega_r}\right)_{a} \bmod 1\right] \qquad \left(\frac{\omega_f}{\omega_r}\right)_{a} \bmod 1 > \frac{1}{2} \tag{98}$$

in equation (95).

Consider now the case when L is odd and $n = (L-1)/2$. Then the set u frequencies are associated with

$$\kappa = \kappa_u < \frac{N}{2} - \frac{\omega_f}{\omega_r}$$

and the set a with

$$\kappa = \kappa_a > \frac{N}{2} - \frac{\omega_f}{\omega_r}$$

Therefore, for $n = n_u = (L-1)/2$ and $\kappa = \kappa_a$,

$$\bar{\mathcal{G}}_{a_{\kappa,n}} = \left(\bar{\mathcal{F}}'_{a_{\kappa,n}}\right)\left(\bar{\mathcal{F}}_{a_{\kappa,n}}\right)^* = \left(\bar{F}'^*_{u_{\kappa,n}}\right)\left(\bar{F}^*_{u_{\kappa,n}}\right)^* = \left(\bar{F}'_{u_{\kappa,n}}\right)^*\left(\bar{F}_{u_{\kappa,n}}\right)$$

$$= \left|\bar{F}_{u_{\kappa,n}}\right|^2 e^{-i2\pi[\kappa_a \Delta\nu/LN + (L-1)\Delta l/2L]} = \left|\bar{\mathcal{G}}_{a_{\kappa,n}}\right| e^{i\gamma_{a_{\kappa,n}}}$$

where use was made of equation (76). Hence

$$\gamma_{a_{\kappa,n}} + 2\pi j_{a_{\kappa,n}} = -2\pi\left(\kappa_a \frac{\Delta\nu}{LN} + \frac{L-1}{2}\frac{\Delta l}{L}\right) \tag{99}$$

and from equation (78), with $n = (L-1)/2$, $\kappa = \kappa_u$,

$$\gamma_{u_{\kappa,n}} + 2\pi j_{u_{\kappa,n}} = 2\pi\left(\kappa_u \frac{\Delta\nu}{LN} + \frac{L-1}{2}\frac{\Delta l}{L}\right) \tag{100}$$

If the selected complex amplitude from the spectrum is incorrectly associated with set u,

$$\gamma_{\dot{u}_{\kappa,n}} = \gamma_{a_{\kappa,n}}$$

Using equations (99) and (100) (with $\dot{u}$ replacing u) in the preceding equation gives

$$\kappa_{\dot{u}} = -\kappa_a + N\frac{\Delta j_{\kappa,n} - (L-1)\Delta l/L}{\Delta m + \Delta l/L} \tag{101}$$

where $\Delta j_{\kappa,n} = j_{\dot{u}_{\kappa,n}} - j_{a_{\kappa,n}}$. On the other hand (eq. (85))

$$\dot{u}_{\kappa,n} = \kappa_{\dot{u}} + \left(\frac{\omega_f}{\omega_r}\right)_{\dot{u}} + \frac{L-1}{2}N \tag{102}$$

Equating now $\dot{u}_{\kappa,n}$ and $a_{\kappa,n}$, given by equation (55), results in

$$\kappa_{\dot{u}} + \left(\frac{\omega_f}{\omega_r}\right)_{\dot{u}} + \frac{L-1}{2}N = -\kappa_a - \left(\frac{\omega_f}{\omega_r}\right)_{a} + \frac{L+1}{2}N$$

and

$$\left(\frac{\omega_f}{\omega_r}\right)_{\dot{u}} = N - (\kappa_{\dot{u}} + \kappa_a) - \left(\frac{\omega_f}{\omega_r}\right)_{a}$$

which is identical to equation (91). Hence, by comparing equations (101) and (89) and referring to equation (93), it follows that for the case $n = (L-1)/2$ the previously derived equations, (94) to (98), will apply provided that

$$\Gamma = N\frac{\Delta j_{\kappa,n} - (L-1)\Delta l/L}{\Delta m + \Delta l/L} \tag{103}$$

This case is significant in particular for $L = 1$ (and therefore $\Delta l = 0$) since it also applies for the discrete blade displacement field.

Note that if the selected complex amplitude were incorrectly assigned to the set a rather than to the set u, subscripts a and $\dot{u}$ would need to be replaced by $\dot{a}$ and u in the preceding equations. These equations would then lead to similar results and conclusions as in the previous case.

Having derived Γ for all n, it is necessary to obtain the range for $\Delta j_{\kappa,n}$'s so that appropriate Γ's can be evaluated for any given choice of Δm and Δl. As discussed previously in connection with equations (92) to (98), it is desirable that $\Gamma \bmod 1 \neq 0$. Using equations (86), (92), and (93) (or alternatively (103), if $n = (L-1)/2$), it follows that

$$-1<\Gamma/N<1 \tag{104}$$

This equation will be satisfied for appropriate Γ's provided $\Delta j_{\kappa,n}$ is within the following limits:

$$\left.\begin{aligned} &-(\Delta m-1)\le\Delta j_{\kappa,n}\le\Delta m-1 && \Delta l=0\\ &-\Delta m+\Delta\le\Delta j_{\kappa,n}\le\Delta m-1+\Delta && \Delta l/L\le 1/2\\ &-(\Delta m+1)+\Delta\le j_{\kappa,n}\le\Delta m-1+\Delta && \Delta l/L>1/2 \end{aligned}\right\} \tag{105}$$

where

$$\Delta=0 \qquad n\neq(L-1)/2$$

$$\Delta=\Delta l \qquad n=(L-1)/2$$

Note that if $\Delta l\neq 0$, $\Gamma\neq 0$ for the preceding $\Delta j_{\kappa,n}$. However, if $\Delta l=0$, equation (96) results for $\Delta j_{\kappa,n}=0$, and therefore no distinction is possible between sets u and a. (The distinction between these sets when $\Delta l=0$ would be possible only if the upper limit in inequality (86) is replaced by $N/2$.)

Equation (93) or (103) should be evaluated for all possible $\Delta j_{\kappa,n}$'s given by equations (105). However, this procedure can be somewhat simplified at the expense of introducing another restriction. From equation (93) it follows that

$$\Gamma \bmod 1=\frac{[N(L\,\Delta j_{\kappa,n}+\Delta l)]\bmod \Delta\nu}{\Delta\nu}$$

Therefore $\Gamma \bmod 1\neq 0$ if

$$\begin{aligned}&[N(L\,\Delta j_{\kappa,n}+\Delta l)]\bmod\Delta\nu\\ &\quad=[N\bmod\Delta\nu(L\,\Delta j_{\kappa,n}+\Delta l)\bmod\Delta\nu]\bmod\Delta\nu\\ &\quad=[N\bmod\Delta\nu(L\,\Delta j_{\kappa,n}+\Delta l)]\bmod\Delta\nu\neq 0\end{aligned} \tag{106}$$

in view of equations (105). It is therefore necessary that

$$N\bmod\Delta\nu\neq 0$$

If in addition $\Delta\nu$ is a prime number, the product of any of the factors of $N \bmod \Delta\nu$ and $(L\,\Delta j_{\kappa,n}+\Delta l)<\Delta\nu$ cannot equal $\Delta\nu$, and therefore $\Gamma \bmod 1$ will not be zero. To summarize, $\Gamma \bmod\neq 0$ if

$$\Delta l\neq 0$$

$$N\bmod\Delta\nu\neq 0 \quad\text{and}\quad \Delta\nu=\text{prime number} \tag{107}$$

Note, however, that the last condition on $\Delta\nu$ is sufficient but not necessary. Equations (107) also hold for $n=(L-1)/2$ when L is odd. If $L=1$, Δl must equal zero and $\Gamma \bmod 1\neq 0$ cannot be satisfied for all $\Delta j_{\kappa,n}$. However, as will be shown later, even for $L=1$ it is possible to choose transducer separation $\Delta\Phi$ so that $\Gamma \bmod 1\neq 0$.

Having determined conditions which guarantee that the selected amplitude will be correctly assigned to either set u or a, there remains to be determined the condition under which there exists only one $j_{\kappa,n}$ and therefore only one κ in either set u or set a.

Let $(k_u)_T$ and $(\omega_f/\omega_r)_T$ in the following equations denote the true values for these variables. Depending on the values of $j_{u_{\kappa,n}}$, there may be several other values of κ and ω_f/ω_r satisfying the appropriate equations. Then for every such $\kappa=(\kappa_u)_F$ and $\omega_f/\omega_r=(\omega_f/\omega_r)_F$,

$$(u_{\kappa,n})_T=(u_{\kappa,n})_F$$

or

$$\left(\frac{\omega_f}{\omega_r}\right)_T+(\kappa_u)_T+n_uN=\left(\frac{\omega_f}{\omega_r}\right)_F+(\kappa_u)_F+n_uN$$

so that

$$(\kappa_u)_T-(\kappa_u)_F=-\left[\left(\frac{\omega_f}{\omega_r}\right)_T-\left(\frac{\omega_f}{\omega_r}\right)_F\right] \tag{108}$$

Because $0<\omega_f/\omega_r<N$, it follows from equation (108) that

$$|(\kappa_u)_T-(\kappa_u)_F|<N \tag{109}$$

On the other hand, from equation (83) it follows that

$$(\kappa_u)_T-(\kappa_u)_F=\frac{LN}{\Delta\nu}\left[\left(j_{u_{\kappa,n}}\right)_T-\left(j_{u_{\kappa,n}}\right)_F\right]=\delta j_{\kappa,n}\frac{N}{\Delta m+\Delta l/L} \tag{110}$$

where use was made of the fact that $(\gamma_{u_{\kappa,n}})_T=(\gamma_{u_{\kappa,n}})_F$ and the definition

$$\delta j_{\kappa,n}=\left(j_{u_{\kappa,n}}\right)_T-\left(j_{u_{\kappa,n}}\right)_F$$

Consequently, in view of equation (109),

$$\left|\frac{\delta j_{\kappa,n}}{\Delta m+\Delta l/L}\right|<1 \tag{111}$$

and therefore

$$\left.\begin{aligned} &|\delta j_{\kappa,n}|\le\Delta m-1 && \Delta l=0\\ &|\delta j_{\kappa,n}|\le\Delta m && \Delta l>0 \end{aligned}\right\} \tag{112}$$

Applying the mod 1 function to the absolute values of the left and right sides of equation (110) results in

$$\left|(\kappa_u)_T-(\kappa_u)_F\right| \bmod 1=\left|\frac{N\delta j_{\kappa,n}}{\Delta m+\Delta l/L}\right| \bmod 1=0$$

because both κ's are integers. Thus multiple solutions for κ will be ruled out if the right side of this equation is zero only when $\delta j_{\kappa,n}=0$. It is necessary therefore that

$$\left[\frac{N|\delta j_{\kappa,n}|}{\Delta m+\Delta l/L}\right] \bmod 1\neq 0 \tag{113}$$

for the nonzero values of $|\delta j_{\kappa,n}|$ given by equation (112).

To derive a simplified condition on Δm and Δl, analogous to condition (107), equation (113) is transformed as follows:

$$\left|(\kappa_u)_T-(\kappa_u)_F\right| \bmod 1=\frac{(NL|\delta j_{\kappa,n}|)\bmod \Delta\nu}{\Delta\nu}=0$$

Therefore

$$\begin{aligned}(NL|\delta j_{\kappa,n}|)\bmod\Delta\nu&=\left[N\bmod\Delta\nu(L|\delta j_{\kappa,n}|)\bmod\Delta\nu\right]\bmod\Delta\nu\\&=\left[N \bmod \Delta\nu(L|\delta j_{\kappa,n}|)\right]\bmod \Delta\nu=0\end{aligned} \tag{114}$$

where use was made of equation (111). Using the same reasoning as in the derivation of equation (107), it follows that if

$$N\bmod\Delta\nu\neq 0 \quad \text{and} \quad \Delta\nu=\text{prime number} \tag{115}$$

$|\delta j_{\kappa,n}|$ must be zero and the solution for κ within set u is unique. As for equations (107), the second requirement on $\Delta\nu$ in equations (115) is more restrictive than necessary. Note that equations (115) and (107) are identical except for the additional requirement, $\Delta l\neq 0$, in equations (107). Conditions (114) and (115) also hold for set a and for $n=(L-1)/2$ when L is odd. If $L=1$ or $\Delta l=0$, conditions (115) are replaced by

$$N\bmod\Delta m\neq 0 \quad \text{and} \quad \Delta m=\text{prime number} \tag{116}$$

As mentioned previously, for the determination of κ it is necessary to assume j. It is useful therefore to derive the plausible limits on j. Applying the limits on ω_f/ω_r to equation (48) gives for both sets of frequencies

$$-(N-1)\leq\kappa\leq N-1 \tag{117}$$

Substituting these limits and the following limit on γ (for either $\gamma=\gamma_u$ or $\gamma=\gamma_a$)

$$0\leq\frac{\gamma_{\kappa,n}}{2\pi}\leq\frac{N-1}{N} \tag{118}$$

in equation (83) or (82) results in

$$-\frac{N-1}{N}\left(\frac{\Delta\nu}{L}+1\right)+n\frac{\Delta l}{L}\leq j_{\kappa,n}\leq\frac{N-1}{N}\frac{\Delta\nu}{L}+n\frac{\Delta l}{L} \tag{119}$$

where again either subscript u or a could be used. If $\Delta l=0$, equation (119) reduces to

$$-\frac{N-1}{N}(\Delta m+1)\leq j_{\kappa,n}\leq\frac{N-1}{N}\Delta m \tag{120}$$

or, since $\Delta m\leq N-1$

$$-\Delta m\leq j_{\kappa,n}\leq\Delta m-1 \tag{121}$$

For odd L, $n=(L-1)/2$, and odd N the limits on κ from equations (29) to (32) are

$$-(N-1)\leq\kappa_u\leq\begin{cases}\dfrac{N-1}{2}, \left(\dfrac{\omega_f}{\omega_r}\right)_u \bmod 1<\dfrac{1}{2}\\[2ex]\dfrac{N-3}{2}, \left(\dfrac{\omega_f}{\omega_r}\right)_u \bmod 1>\dfrac{1}{2}\end{cases} \tag{122}$$

$$\left.\begin{aligned}&\left(\frac{\omega_f}{\omega_r}\right)_a \bmod 1<\frac{1}{2}, -\frac{N-3}{2}\\&\left(\frac{\omega_f}{\omega_r}\right)_a \bmod 1>\frac{1}{2}, -\frac{N-1}{2}\end{aligned}\right\}\leq\kappa_a\leq N-1 \tag{123}$$

Therefore, using equations (99) and (100), for odd N

$$\left.\begin{aligned}&-\frac{N-1}{N}\left(\frac{\Delta\nu}{L}+1\right)\pm\frac{L-1}{2}\frac{\Delta l}{L}\leq j_{\kappa,n}\\&\qquad\frac{1}{2}\frac{N-1}{N}\frac{\Delta\nu}{L}\pm\frac{L-1}{2}\frac{\Delta l}{L}\geq j_{\kappa,n}\\&\left(\frac{\omega_f}{\omega_r}\right)_u \bmod 1<\frac{1}{2}, \left(\frac{\omega_f}{\omega_r}\right)_a \bmod 1>\frac{1}{2},\\&\qquad\frac{1}{2}\frac{N-3}{N}\frac{\Delta\nu}{L}\pm\frac{L-1}{2}\frac{\Delta l}{L}\geq j_{\kappa,n}\\&\left(\frac{\omega_f}{\omega_r}\right)_u \bmod 1>\frac{1}{2}, \left(\frac{\omega_f}{\omega_r}\right)_a \bmod 1<\frac{1}{2},\end{aligned}\right\} \tag{124}$$

Where the positive sign is to be used for set u and the minus sign for set a. For $n=(L-1)/2$ and even N from equations (27) and (28) it follows that

$$\left.\begin{aligned} -(N-1) \le \kappa_u \le \frac{N}{2} - 1 \\ -\left(\frac{N}{2} - 1\right) \le \kappa_a \le N-1 \end{aligned}\right\} \tag{125}$$

and

$$-\frac{N-1}{N}\left(\frac{\Delta\nu}{L}+1\right) \pm \frac{L-1}{2}\frac{\Delta l}{L} \le j_{\kappa,n} \le \frac{1}{N}\left(\frac{N}{2}-1\right)\frac{\Delta\nu}{L} \pm \frac{L-1}{2}\frac{\Delta l}{L} \tag{126}$$

where the signs are to be used as in equation (124). If $\Delta l = 0$ and $n = (L-1)/2$

$$-\Delta m \le j_{\kappa,n} \le \begin{cases} \dfrac{\Delta m}{2} - 1 & \Delta m \text{ even} \\ \dfrac{\Delta m - 1}{2} & \Delta m \text{ odd} \end{cases} \tag{127}$$

provided that $\Delta m \le N/2$ for even N and $\Delta m \le N/3$ for odd N. These limits are also applicable for the $L = 1$ case of blade displacements.

The general procedure for finding κ and ω_f/ω_r associated with the particular $\bar{G}_{\kappa,n}$ can now be described. Given the measured values of $\gamma_{\kappa,n}$, $u_{\kappa,n}$ (or $a_{\kappa,n}$) and (ω_f/ω_r) mod 1, first compute the possible κ_u's and κ_a's from equation (83) or (82) using j's given by any one of equations (119), (121), (124), (126), or (127). Reject κ's that are nonintegral and for each integral κ compute ω_f/ω_r from equations (85) and (90). Reject those κ's for which (ω_f/ω_r) mod 1 does not correspond to the measured value or for which ω_f/ω_r does not satisfy inequality (86). The remaining κ's should all be associated with either the set u only or the set a only. If the transducer spacing was chosen so that Γ mod $1 \neq 0$ for the appropriate Γ, there will remain only one κ for which the associated ω_f/ω_r is between 0 and N.

When sampling blade displacements and the transducer separation $\Delta\Phi$ is such that

$$\delta\Phi = \Delta\Phi \bmod \left(\frac{2\pi}{N}\right) \neq 0 \tag{128}$$

before taking the cross-power spectrum, one must compensate for the fact that at the time $t = 0$, when the blade $m = 0$ is aligned with the first transducer, no blade is aligned with the second transducer. The next available blade (i.e., $m = \Delta m + 1$) will reach the second transducer after the time period

$$\frac{2\pi/N - \delta\Phi}{\omega_r}$$

(Note that $\Delta\Phi$ and Δm increase in the direction opposite to the rotation.) Hence one must introduce the corresponding phase angle correction in the transform of the second transducer. Therefore

$$\begin{aligned} |\bar{G}_{u_\kappa}|\, e^{i\tilde{\gamma}_{u_\kappa}} &= (\bar{\alpha}'_{u_\kappa})(\bar{\alpha}_{u_\kappa})^* = \left(\bar{\alpha}_{u_\kappa}\, e^{i(\omega_f/\omega_r)(2\pi/N-\delta\Phi)} \times e^{i2\pi\kappa_u(\Delta m+1)/N}\right)(\bar{\alpha}_{u_\kappa})^* \\ &= (\bar{A}_{u_\kappa})(\bar{A}^*_{u_\kappa})\, e^{i(\omega_f/\omega_r)(2\pi/N-\delta\Phi)} \times e^{i2\pi\kappa_u(\Delta m+1)/N} = |\bar{G}_{u_\kappa}|\, e^{i\gamma_{u_\kappa}} \end{aligned}$$

and

$$\tilde{\gamma}_{u_\kappa} + 2\pi j_{u_\kappa} = \left(\frac{\omega_f}{\omega_r}\right)_u \left(\frac{2\pi}{N} - \delta\Phi\right) + 2\pi\kappa_u \frac{\Delta m + 1}{N} \tag{129}$$

where $\tilde{\gamma}_{u_\kappa}$ is the measured phase angle, which is distinct from the true cross-power phase γ_{u_κ}

$$\tilde{\gamma}_{u_\kappa} = \gamma_{u_\kappa} + \left(\frac{\omega_f}{\omega_r}\right)\left(\frac{2\pi}{N} - \delta\Phi\right)$$

The corresponding equation for the set a is

$$\tilde{\gamma}_{a_\kappa} + 2\pi j_{a_\kappa} = -\left(\frac{\omega_f}{\omega_r}\right)_a \left(\frac{2\pi}{N} - \delta\Phi\right) - 2\pi\kappa_a \frac{\Delta m + 1}{N} \tag{130}$$

The equations

$$\dot{u}_\kappa = a_\kappa,\ \tilde{\gamma}_{\dot{u}_\kappa} = \tilde{\gamma}_{a_\kappa}$$

together with equations (14), (20), (129), and (130) can now be used to obtain

$$\left(\frac{\omega_f}{\omega_r}\right)_{\dot{u}} = N - \left(\frac{\omega_f}{\omega_r}\right)_a - N\frac{\Delta j_\kappa - 1 + \delta\Phi/(2\pi/N)}{\Delta m + \delta\Phi/(2\pi/N)} \tag{131}$$

where $\Delta j_\kappa = j_{\dot{u}_\kappa} - j_{a_\kappa}$. Comparison of equation (92) with the preceding then leads to the appropriate Γ,

$$\Gamma = N\frac{\Delta j_\kappa - 1 + \delta\Phi/(2\pi/N)}{\Delta m + \delta\Phi/(2\pi/N)} \tag{132}$$

For the same reasons discussed in connection with equations (92) to (98),

Γ mod $1 \neq 0$

to correctly associate a particular complex amplitude with either set u or set a.

The limits on Δj_κ in equation (132) can again be derived by using equation (104). Thus

$$\left.\begin{aligned} &-(\Delta m-2)\le\Delta j_\kappa\le\Delta m && \delta\Phi=0\\ &-(\Delta m-1)\le\Delta j_\kappa\le\Delta m && \frac{\delta\Phi}{(2\pi/N)}\le\frac{1}{2}\\ &-\Delta m\le\Delta j_\kappa\le\Delta m && \frac{\delta\Phi}{(2\pi/N)}>\frac{1}{2} \end{aligned}\right\} \quad (133)$$

If $\delta\Phi=0$, for $\Delta j_\kappa=1$, $\Gamma=0$ and thus $\Gamma \bmod 1=0$. It is therefore desirable that $\delta\Phi$ not be zero (otherwise eq. (86) should be replaced by $0<\omega_f/\omega_r<N/2$). If $\delta\Phi$ is not equal to zero, equation (133) should be used to verify that $\Gamma \bmod 1$ is not zero for a particular choice of Δm and $\delta\Phi$. However, if $\delta\Phi/(2\pi/N)$ can be expressed as a ratio of two integers, that is

$$\left.\begin{aligned} &\frac{\delta\Phi}{(2\pi/N)}=\frac{\Delta l}{L}\\ &\text{and}\\ &\frac{\Delta\Phi}{(2\pi/N)}=\frac{\Delta\nu}{L} \end{aligned}\right\} \quad (134)$$

equations (107) will insure that $\Gamma \bmod 1\neq 0$. (Note that here $\Delta l, \Delta\nu$, and L are used only to define $\delta\Phi$ and $\Delta\Phi$ and that L does not indicate number of samples per blade passage during sampling.)

As in the previous case, one must also insure that there is only one solution for κ in a given set (u or a). The expression

$$(\kappa_u)_T-(\kappa_u)_F=\frac{N\delta j_\kappa}{\Delta m+\delta\Phi/(2\pi/N)} \qquad \delta j_\kappa=(j_{u_\kappa})_T-(j_{u_\kappa})_F$$

can be derived similarly to equation (110). To satisfy equation (86),

$$\frac{|\delta j_\kappa|N}{\Delta m+\delta\Phi/(2\pi/N)}<1$$

and

$$\left.\begin{aligned} &|\delta j_\kappa|\le\Delta m-1 && \delta\Phi=0\\ &|\delta j_\kappa|\le\Delta m && \delta\Phi\neq 0 \end{aligned}\right\} \quad (135)$$

Therefore κ will be unique within a given set if $\Delta\Phi$ is such that

$$\left[\frac{N|\delta j_\kappa|}{\Delta m+\delta\Phi/(2\pi/N)}\right]\bmod 1\neq 0 \qquad \delta j_\kappa\neq 0 \quad (136)$$

The possible nonzero values for δj_κ are given by inequalities (135). If $\delta\Phi/(2\pi/N)$ and $\Delta\Phi/(2\pi/N)$ can be expressed by equation (134), it is sufficient to satisfy conditions (116) instead of (136). Equations (116) and (136) also apply for set a.

In this case the estimates for j_{u_κ} and j_{a_κ} are given by

$$\left.\begin{aligned} -\frac{N-1}{N}(\Delta m+2)\le j_{u_\kappa}\le\frac{1}{2}\left(\frac{N-1}{N}\right)(\Delta m+1)\\ +\left(1-\frac{\delta\Phi}{2\pi/N}\right)\\ -\left(1-\frac{\delta\Phi}{2\pi/N}\right)-\frac{N-1}{N}(\Delta m+2)\le j_{a_\kappa}\\ \le\frac{1}{2}\left(\frac{N-1}{N}\right)(\Delta m+1) \end{aligned}\right\} \quad (137)$$

These inequalities can be derived by using equations (122), (123), (129), and (130).

The flutter frequency can also be obtained by using the individual blade spectra. The phase angle difference between the two transducers based on the individual blade spectra of a single blade is related to the flutter frequency and the angular transducer separation as follows:

$$\left.\begin{aligned} \phi_m-\phi'_m+2\pi j_u=\left(\frac{\omega_f}{\omega_r}\right)_u\Delta\Phi\\ 0\le\frac{\phi_m-\phi'_m}{2\pi}<1\\ -(\phi_m-\phi'_m)-2\pi j_a=\left(\frac{\omega_f}{\omega_r}\right)_a\Delta\Phi \end{aligned}\right\} \quad (138)$$

where again the prime is used to associate a variable with the second transducer. The expression for the erroneously assigned (to the set u) flutter frequency is then

$$\left(\frac{\omega_f}{\omega_r}\right)_{\dot{u}}=-\left(\frac{\omega_f}{\omega_r}\right)_a+\frac{N}{\Delta m+\delta\Phi/(2\pi/N)}\Delta j$$

$$=N-\left(\frac{\omega_f}{\omega_r}\right)_a-\left[1-\frac{\Delta j}{\Delta m+\delta\Phi/(2\pi/N)}\right]N$$

where $\delta\Phi$ is given by equation (128) and $\Delta j=j_{\dot{u}}-j_a$. Comparing equation (92) with the preceding gives

$$\Gamma=\left[1-\frac{\Delta j}{\Delta m+\delta\Phi/(2\pi/N)}\right]N \quad (139)$$

To be able to associate a selected complex amplitude with either set u or set a, it is necessary for $\delta\Phi$ to be such that

$\Gamma \bmod 1 \neq 0$. The ranges for Δj to be used in the expression for Γ can be obtained from equation (138) by applying inequality (86). They are

$$\left.\begin{array}{ll} 1 \leq \Delta j \leq 2\Delta m - 1 & \delta\Phi = 0 \\ 1 \leq \Delta j \leq 2\Delta m & \delta\Phi/(2\pi/N) \leq 1/2 \\ 1 \leq \Delta j \leq 2\Delta m + 1 & \delta\Phi/(2\pi/N) > 1/2 \end{array}\right\} \quad (140)$$

Since $\Gamma = 0$ when $\delta\Phi = 0$ and $\Delta j = \Delta m$, $\delta\Phi$ should not be zero. Provided $\delta\Phi/(2\pi/N)$ and $\Delta\Phi/(2\pi/N)$ can be expressed by equations (134), it is sufficient to satisfy conditions (107) to insure that $\Gamma \bmod 1 \neq 0$. However, because one now has to work with frequencies rather than nodal diameters, restrictions (97) and (98) apply.

Assuming again the true and false values for ω_f/ω_r (associated with the true and false values of j_u), equation (138) yields

$$\left(\frac{\omega_f}{\omega_r}\right)_T - \left(\frac{\omega_f}{\omega_r}\right)_F = \frac{\delta j_u}{\Delta\Phi/2\pi} = \frac{N}{\Delta m + \delta\Phi/(2\pi/N)}\delta j_u \quad (141)$$

where $\delta j_u = (j_u)_T - (j_u)_F$. In view of the limits imposed on ω_f/ω_r,

$$\left|\left(\frac{\omega_f}{\omega_r}\right)_T - \left(\frac{\omega_f}{\omega_r}\right)_F\right| = \left|\frac{\delta j_u}{\Delta m + \delta\Phi/(2\pi/N)}\right| N < N \quad (142)$$

and

$$\left.\begin{array}{ll} |\delta j_u| \leq \Delta m & \delta\Phi > 0 \\ |\delta j_u| \leq \Delta m - 1 & \delta\Phi = 0 \end{array}\right\} \quad (143)$$

Since the left side of equation (142) must be a positive integer,

$$\left|\left(\frac{\omega_f}{\omega_r}\right)_T - \left(\frac{\omega_f}{\omega_r}\right)_F\right| \bmod 1 = \left[\frac{|\delta j_u| N}{\Delta m + \delta\Phi/(2\pi/N)}\right] \bmod 1 = 0$$

Therefore, to have a single solution for ω_f/ω_r within set u, equation (136) must be satisfied with δj_u replacing δj_κ. The nonzero values for $|\delta j_u|$ are given by inequalities (143). This procedure also holds for set a. If the angular separation between two transducers can be expressed by equations (134), condition (116) can be used instead of (137). As for Γ, for this sampling rate there is an additional restriction

$$\left[\frac{|\delta j_u| N}{\Delta m + \delta\Phi/(2\pi/N)}\right] \bmod 1 \neq \begin{cases} 2\left[\left(\frac{\omega_f}{\omega_r}\right)_T \bmod 1\right] & \left(\frac{\omega_f}{\omega_r}\right)_T < \frac{1}{2} \\ 2\left[\left(\frac{\omega_f}{\omega_r}\right)_T \bmod 1\right] - 1 & \left(\frac{\omega_f}{\omega_r}\right)_T > \frac{1}{2} \end{cases} \quad (144)$$

From equations (138) and (86) the estimates for ranges of j_u and j_a are

$$\left.\begin{array}{lll} 0 \leq j_u \leq \Delta m - 1 & -\Delta m \leq j_a \leq -1 & \delta\Phi = 0 \\ 0 \leq j_u \leq \Delta m & -(\Delta m + 1) \leq j_a \leq -1 & \delta\Phi \neq 0 \end{array}\right\} \quad (145)$$

Table I (ref. 2) illustrates the phase relationship between the two pressure transducers 47.4° apart (a distance that corresponded to $\Delta m = 5$). The flutter point was the same as for figures 1 to 3, and therefore the true flutter frequency was 8.45 E. In the axial direction these transducers were located past the blade midchord position. In contrast to the leading-edge location, at this chordwise position there was a significant response for the $n = 0$ harmonic. Consequently a low-pass filter could be used to cut off the response beyond about $\omega_f/\omega_r = 25$. This eliminated the higher harmonics, as well as the dominant part of the steady-state response and considerably simplified the analysis.

In this case the true flutter frequency was known from the blade-mounted strain-gage outputs. Consequently the cross-power phase angles based on the known nodal diameters associated with each frequency in the first column could be computed and tabulated in the last column. Comparing these phase angles with the measured phase angles in the second column indicates a particularly satisfactory agreement for the backward-traveling waves.

TABLE I. – PHASE RELATIONSHIPS BETWEEN TWO TRANSDUCERS 47.4° APART

Frequency, engine orders	Cross-power-spectrum phase, deg	Phase based on κ, deg
3.45	122.0	123.0
4.45	173.6	170.5
5.45	215.8	217.9
6.43	266.3	265.3
8.44	256.7	0
11.46	150.0	142.1
12.45	201.7	189.5

To illustrate the procedure presented in this section, flutter frequency will assumed to be unknown now, and the measured cross-power phase associated with the 5.45 E response will be used to determine it. Note that $\Delta l=0$, $\Delta m=5$ is a prime number, and, for $N=38$, $N \bmod \Delta m=3\neq 0$. Therefore condition (116) is satisfied; however, condition (107) is not. From equation (121), $-5<\Delta j_{\kappa,n}<4$. For these j's equation (83) yields two values of κ_u that are close to being integers, $\kappa_u=-3.04\sim -3$ (for $j_{\kappa,n}=-1$) and $\kappa_u=34.96\sim 35$ (for $j_{\kappa,n}=4$). For these κ's from equation (53) $\omega_f/\omega_r=8.45$ and -29.55. The last value associated with $\kappa_u=35$ must be ruled out. From equation (82), the other two possible values of κ's (corresponding to the same values of $j_{\kappa,n}$) are $\kappa_a=3.04\sim 3$ and $\kappa_a=-34.96\sim -35$. For $\kappa_a=-35$ from equation (90) $\omega_f/\omega_r=-2.45$, and therefore this solution must also be ruled out. However, for $\kappa_a=3$, $\omega_f/\omega_r=29.55$, which is within the assumed limits given by inequality (86). Without further input therefore it is impossible to determine the correct solution. Had the determination of frequency been the primary object, a better choice for second transducer location would be the one that satisfies condition (107). In particular this condition requires that $\Delta l\neq 0$.

Interaction with Steady-State Pressure

The true fluctuating pressure on the blade surface must be defined in terms of the coordinate system (ξ,η) fixed with respect to a blade, figure 5. The coordinate system (x,y) in this figure is fixed with respect to the rotor, and the x coordinate is measured from the undeflected position of blade $m=0$ along the outer circumference of the rotor. The instantaneous displacement of the m^{th} blade in the (x,y) coordinate system is given by δx_m; and the undeflected blade position, by x_m.

For the m^{th} blade the pressure measured by a stationary sensor $P_{t,m}$ can be expressed as a sum of the unsteady pressure $P_m(\xi,t)$ and the steady-state pressure $P_{s,m}(\xi)$; that is,

$$P_{t,m}=P_m(\xi,t)+P_{s,m}(\xi) \qquad |\xi|<<\frac{1}{2}R\frac{2\pi}{N} \tag{146}$$

where the condition on ξ implies that the pressure distributions are restricted to the immediate neighborhood of a blade. Both positive and negative ξ's are allowed. It is also assumed that the blade displacements are much smaller than the blade spacing.

After the coordinate transformation

$$x-x_m=\xi+\delta x_m(t) \tag{147}$$

is introduced, equation (146) becomes

$$P_{t,m}=P_m(x-x_m-\delta x_m,t)+P_{s,m}(x-x_m-\delta x_m) \tag{148}$$

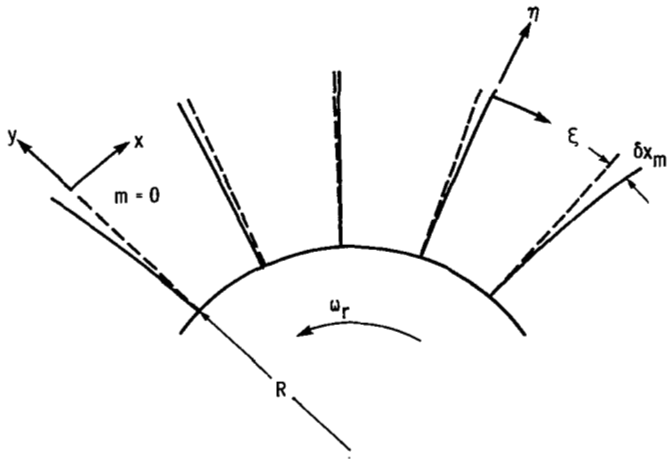

Figure 5. – Definition of (ξ,η) and (x,y) coordinate systems.

In the (x,y) coordinate system, both P_m and $P_{s,m}$ depend on blade displacement δx_m. Expanding equation (148) in powers of δx_m to first-order results in

$$P_{t,m}\sim P_m(x-x_m,t)+P_{s,m}(x-x_m)-\left.\frac{\partial P_m}{\partial x}\right|_{\delta x=0} \times \delta x_m-\left.\frac{dP_{s,m}}{dx}\right|_{\delta x=0}\delta x_m \tag{149}$$

$$|x-x_m|<<R\pi/N$$

where the derivatives are evaluated for $\delta x_m=0$. Since it is expected that $P_m<<P_{s,m}$,

$$\left.\frac{\partial P_m}{\partial x}\right|_{\delta x=0}<<\left.\frac{dP_{s,m}}{dx}\right|_{\delta x=0}$$

and

$$P_{t,m}\sim P_m(x-x_m,t)+P_{s,m}(x-x_m)-\left.\frac{dP_{s,m}}{dx}\right|_{\delta x=0}\delta x_m \tag{150}$$

Transformation into a stationary reference frame by using the real part of equation (11) with $\psi_k=\psi_{\delta x,k}$ and $\bar{A}_k=\bar{A}_{\delta x,k}$ and the real part of $\hat{\alpha}$ replaced by δx_m results in

$$P_t\sim P(\mu)+P_s(\mu)-\left.\frac{dP_s}{dx}\right|_{\delta x=0}\sum_{k=0}^{N-1}|\bar{A}_{\delta x,k}| \times\cos\left[\left(\frac{\omega_f}{\omega_r}+k\right)\frac{2\pi}{N}(m+qN)+\psi_{\delta x,k}\right] \tag{151}$$

$$|\mu-\mu_m|\leq\epsilon<<\frac{L}{2} \quad\text{or}\quad |\mu-mL|\leq\epsilon+qLN<<\frac{L}{2}+qLN$$

where μ is defined by equations (36) and (37). When $L=1$, $P(\mu)$ is given by the real part of equation (11) (in which case P, P_s, and $(dP_s/dx)|_{\delta x=0}$ become functions of $m+qN$). When $L>1$, $P(\mu)$ is given by the real part of equation (47). The third term in equation (151) is proportional to the steady-state gradient evaluated for $\delta x_m=0$. In the (x,y) coordinate system, it represents an apparent unsteady pressure component that is created by the displacement of the steady-state pressure field. Because the steady-state pressure gradient is expected to be much smaller away from the immediate neighborhood of a blade, the contribution of this term can be neglected to a first approximation in this region. Therefore

$$P_t \sim P(\mu)+P_s(\mu) \text{ for } |\mu-mL|>\epsilon+qLN,\ L>1$$

Also, to properly use equation (151), it is assumed that m is incremented in the last term when $\mu-\mu_m=-|\epsilon|$ and not 0. The pressure P is now defined for all ranges of μ when $L>1$.

If data are sampled over Q revolutions and then arranged into a matrix so that each row starts at a fixed $\nu=\nu_0$ $(L>1)$ or $m=m_0$ $(L=1)$ and contains either LN $(L>1)$ or N $(L=1)$ samples, the phase angles associated with each row (i.e., each revolution) will be random for the first and third terms in equation (151) and constant for the second term in this equation. This follows from the fact that all harmonics for the first term (eqs. (11) and (47)) and the third term contain a nonintegral shift $\pm\omega_f/\omega_r$, whereas the second term originates from the steady-state term and therefore all harmonics for this term are of integral engine orders. Therefore, by averaging Q rows, column by column, the contribution of first and third terms will be essentially eliminated and only the contribution of the second term in equation (151) will remain. This presents a way of eliminating the steady-state contribution from the spectrum. Averaging is most conveniently performed in the time domain by using the once-per-revolution trigger to mark each revolution (i.e., fix ν_0 or m_0). (Note that revolutions for this procedure do not have to be consecutive.) Once the steady-state distribution is obtained in the time domain, it can be subtracted from the total signal for each q and ν (or m) leaving only the unsteady components in the signal. The same procedure is applied for both pressures and displacements with the exception that the third term in equation (151) is nonexistent and only the $L=1$ case is possible for displacement signals.

For the pressure signals it is also desirable to eliminate the contribution of the third term. To do this according to equation (151) would be tedious. However, as will be shown, its presence does not affect stability criteria, and consequently it is not an important contaminant in the spectrum. Also, for $L>1$, when it is desired to obtain pressure amplitude distribution in the blade passage, L is usually selected sufficiently large so that the proportion of samples falling in the range $|\mu-\mu_m|<\epsilon$ can be counted to be small. Some other ways of minimizing the contribution of this term when blade surface pressures are desired and $L=1$ are discussed in reference 3.

Figure 6 illustrates a linear pressure spectrum for which the steady-state response was not removed before spectral analysis. The flutter point is the same as for figure 4. Comparing magnitudes of the unsteady and the steady-state amplitudes justifies the assumption made in deriving equation (150).

Some experimental evidence regarding the contribution to the unsteady pressure due to the displacement of the steady-state pressure field can be found in reference 3.

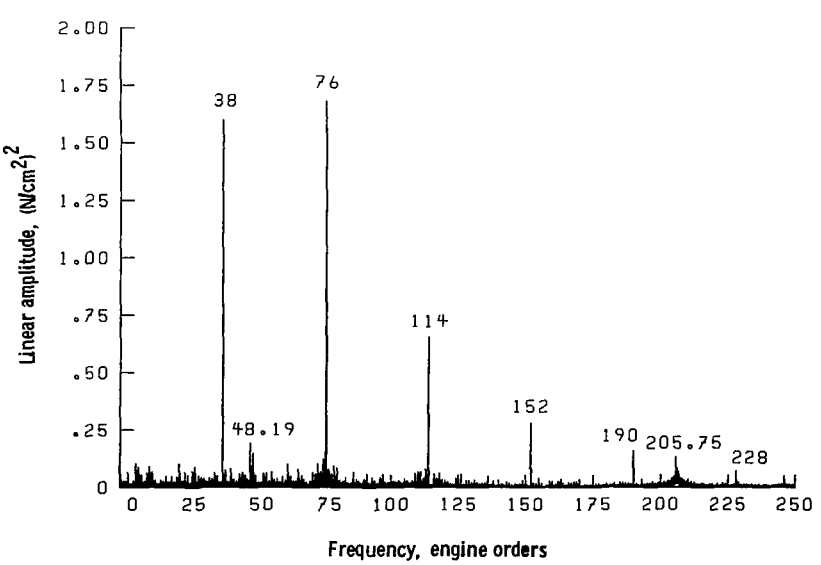

Figure 6. – Linear spectrum of leading-edge pressure transducer; integral engine-order harmonics retained; engine B.

Computation of Aerodynamic Work

In case flutter is mistuned and several modes are present, it is of interest to establish which are the least stable modes. If both pressures and displacements are measured, it is possible to do this by computing the aerodynamic work for each mode. For completeness therefore the two-dimensional expressions for aerodynamic work will be derived by using the modal expansions for pressure and displacement (as would be obtained from the overall stationary spectra for these variables). The most frequent case of torsional flutter will be assumed.

Taking the positive direction for the moment to coincide with the positive sense of variation of the θ coordinate in figure 7, the contribution to the moment (per unit span) from the $d\zeta$ element of the chord for the m^{th} blade is

$$d\hat{M}_m = \Delta\hat{P}_m(\chi c - \zeta)\ d\zeta \tag{152}$$

where ΔP_m denotes suction- minus pressure-side unsteady differential pressure, χc is the distance from the leading edge to the torsional axis, and the ζ coordinate is measured from the leading edge along the chord. The differential work can now be obtained by multiplying equation (152) by the differential displacement

$$d\theta_m = \frac{1}{2} d(\hat{\theta}_m + \hat{\theta}_m^*) \tag{153}$$

which results in the differential work

$$\begin{aligned} d^2\hat{W}_m &= \frac{1}{2}\Delta\hat{P}_m d(\hat{\theta}_m + \hat{\theta}_m^*)(\chi c - \zeta)\ d\zeta \\ &= \frac{i}{2}\Delta\bar{P}_m\, e^{i\omega_f t}|\bar{\theta}_m|\left(e^{i(\omega_f t + \phi_{\theta_m})} - e^{-i(\omega_f t + \phi_{\theta_m})}\right) \\ &\qquad \times(\chi c - \zeta)\ d\zeta d(\omega_f t) \\ &= \frac{i}{2}\Delta\bar{P}_m|\bar{\theta}_m|\, e^{-i\phi_{\theta_m}}\left(e^{2i(\omega_f t + \phi_{\theta_m})} - 1\right)(\chi c - \zeta)\ d(\omega_f t) \\ &= \frac{i}{2}\Delta\bar{P}_m\bar{\theta}_m^*\left(e^{2i(\omega_f t + \phi_{\theta_m})} - 1\right)(\chi c - \zeta)\ d\zeta d(\omega_f t) \end{aligned} \tag{154}$$

where ϕ_{θ_m} is the phase associated with $\bar{\theta}_m$. Integrating this expression with respect to $\beta = \omega_f t + \phi_{\theta_m}$ from 0 to 2π gives

$$\begin{aligned} d\hat{W}_m &= \frac{i}{2}\Delta\bar{P}_m\bar{\theta}_m^*(\chi c - \zeta)\ d\zeta \int_0^{2\pi}(e^{2i\beta} - 1)\ d\beta \\ &= -i\pi\Delta P_m\bar{\theta}_m^*(\chi c - \zeta)\ d\zeta \end{aligned} \tag{155}$$

Summing equation (155) over m results in

$$d\hat{W} = -i\pi(\chi c - \zeta)\ d\zeta \sum_{m=0}^{N-1}\Delta\bar{P}_m\bar{\theta}_m^* \tag{156}$$

The summation in this equation can be expressed in terms of DFT's of $\Delta\bar{P}_m$ and $\bar{\theta}_m^*$, which are denoted by $\bar{A}_{\Delta P,k}$ and $\bar{A}_{\theta,k}^*$. Using equation (12) in terms of these variables, with κ substituted for the dummy index k in the sum for $\bar{\theta}_m^*$, it follows that

$$\begin{aligned} \sum_{m=0}^{N-1}\Delta\bar{P}_m\bar{\theta}_m^* &= \sum_{m=0}^{N-1}\sum_{k=0}^{N-1}\sum_{\kappa=0}^{N-1}\bar{A}_{\Delta P,k}\bar{A}_{\theta,\kappa}^*\, e^{i2\pi m(k-\kappa)/N} \\ &= \sum_{k=0}^{N-1}\sum_{\kappa=0}^{N-1}\bar{A}_{\Delta P,k}\bar{A}_{\theta,\kappa}^*\sum_{m=0}^{N-1} e^{i2\pi m(k-\kappa)/N} \end{aligned} \tag{157}$$

Since

$$\sum_{m=0}^{N-1} e^{i2\pi m(k-\kappa)/N}\begin{cases} = 0 & k \neq \kappa \\ = N & k = \kappa \end{cases}$$

equation (157) becomes

$$\sum_{m=0}^{N-1}\Delta\bar{P}_m\bar{\theta}_m^* = N\sum_{k=0}^{N-1}\bar{A}_{\Delta P,k}\bar{A}_{\theta,k}^* \tag{158}$$

Substitution of this identity in equation (156) results in

$$\begin{aligned} d\hat{W} &= -i\pi(\chi c - \zeta)\ d\zeta N\sum_{k=0}^{N-1}\bar{A}_{\Delta P,k}\bar{A}_{\theta,k}^* \\ &= -i\pi(\chi c - \zeta)\ d\zeta N\sum_{k=0}^{N-1}|\bar{A}_{\Delta P,k}|\ |\bar{A}_{\theta,k}|\, e^{i(\psi_{\Delta P,k} - \psi_{\theta,k})} \end{aligned} \tag{159}$$

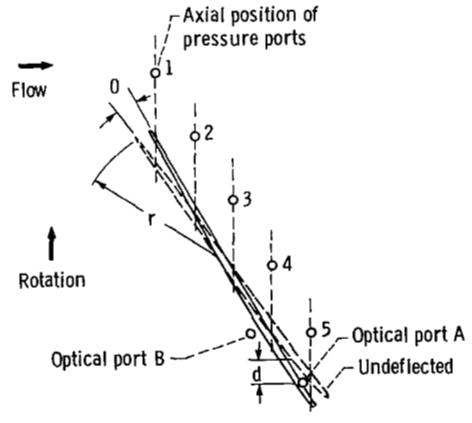

Figure 7. – Location of measurement ports.

and

$$dW=\pi(\chi c-\zeta)N\sum_{k=0}^{N-1}|\bar{A}_{\Delta P,k}|\ |\bar{A}_{\theta,k}|\sin(\psi_{\Delta P,k}-\psi_{\theta,k}) \tag{160}$$

Integration with respect to ζ gives

$$W=\pi N\int_0^c(\chi c-\zeta)\left[\sum_{k=0}^{N-1}|\bar{A}_{\Delta P,k}|\ |\bar{A}_{\theta,k}|\times\sin(\psi_{\Delta P,k}-\psi_{\theta,k})\right]d\zeta \tag{161}$$

or for any particular k

$$W_k=\pi N\int_0^c(\chi c-\zeta)|\bar{A}_{\Delta P,k}|\ |\bar{A}_{\theta,k}|\sin(\psi_{\Delta P,k}-\psi_{\theta,k})\ d\zeta \tag{162}$$

From equations (156) and (159) it follows that only the imaginary parts of the products $\Delta\bar{P}_m\bar{\theta}_m^*$ and $\bar{A}_{\Delta P,k}\bar{A}_{\theta,k}^*$ contribute to aerodynamic work. Frequently the phase of pressure (or moment) is measured relative to the displacement. Then one can state that only the imaginary part of pressure (or moment) contributes to the work. Returning now to equation (151), it can be seen that the third term in this equation is either in phase or π radians out of phase with the displacement (i.e., it is real). It follows therefore that this term has no significance for computation of aerodynamic work and is irrelevant for stability of the system.

Equation (162) is frequently stated in terms of dimensionless imaginary moment coefficient $(C_{M,k})_I$; that is,

$$W_k=\left(\frac{\rho V^2}{2}\right)c^2\pi N|\bar{A}_{\theta,k}|^2(C_{M,k})_I \tag{163}$$

where ρ is the density, V is the relative velocity, and $(C_{M,k})_I$ is given by

$$(C_{M,k})_I=\frac{1}{|\bar{A}_{\theta,k}|}\int_0^1\left(\chi-\frac{\zeta}{c}\right)\frac{\bar{A}_{\Delta P,k}}{\rho V^2/2}\times\sin(\psi_{\Delta P,k}-\psi_{\theta,k})\ d\left(\frac{\zeta}{c}\right) \tag{164}$$

The logical extensions for a mistuned rotor are

$$W=\frac{\rho V^2}{2}c^2\pi N(C_M)_I\sum_{k=0}^{N-1}|A_{\theta,k}|^2 \tag{165}$$

$$(C_M)_I=\frac{1}{\sum_{k=0}^{N-1}|\bar{A}_{\theta,k}|^2}\sum_{k=0}^{N-1}|\bar{A}_{\theta,k}|\int_0^1\left(\chi-\frac{\zeta}{c}\right)\frac{|\bar{A}_{\Delta P,k}|}{\rho V^2/2}\times\sin(\psi_{\Delta P,k}-\psi_{\theta,k})\ d\left(\frac{\zeta}{c}\right)$$

$$=\frac{1}{\sum_{k=0}^{N-1}|\bar{A}_{\theta,k}|^2}\sum_{k=0}^{N-1}|\bar{A}_{\theta,k}|^2(C_{M,k})_I \tag{166}$$

Concluding Remarks

Analytic expressions were developed that describe the displacement and the pressure spectra in a stationary reference frame. The sampling rates considered were the once per revolution, the once per blade, and for the pressure, a multiple of the once per blade. The once-per-revolution sampling involved multiple aliasing and hence appears to be less desirable than the once-per-blade sampling, which resulted in a spectrum that is folded only once. Despite the folding, all N possible modal responses can be easily obtained from this spectrum if the true flutter frequency is known.

Analytic expressions were found to be essential for interpreting a complete pressure-field spectrum, which results when sampling at a rate multiple of the blade passing frequency. A procedure was described that allows the unsteady pressure field to be transformed into a rotating frame of reference yielding the distribution of the unsteady amplitude and phase around the rotor. For this spectrum, also included were the expressions for the nodal diameters. Although the complete pressure-field spectrum was found to be somewhat more difficult to analyze, its advantage is that there is no need to locate the blades in the sampled time domain record. (This step is necessary for the once-per-blade sampling of blade surface pressures.)

Common to all stationary spectra is the fact that the true flutter frequency cannot be determined with a single sensor. A procedure was described that allows its determination by using two sensors. All three sampling rates were considered and the aliased parts of the spectra were included in the analysis.

Equations were derived that illustrate the contribution of the steady-state field to a stationary pressure spectrum.

By using the expression for aerodynamic work, it was shown that stability of the system can be described in terms of the stationary cross-power spectrum between the differential pressure and the displacement.

Lewis Research Center
National Aeronautics and Space Administration
Cleveland, Ohio, November 22, 1983

Appendix – Interpolation Formulas

The formulas presented in this appendix were originally derived by Donald C. Braun of Lewis. They are presented here for completeness. The object of these formulas is to relate the amplitude A_g, the phase θ_g, and the frequency f_g of the cosine function

$$\alpha(t) = A_g \cos(2\pi f_g t + \theta_g) \tag{A1}$$

to the parameters obtainable from the nearest frequency lines in the measured spectrum. (Note that the symbols in the appendix are defined independently of the main text and the symbol list.) However, because different window weighting functions are frequently used in the spectral analysis, the preceding cosine function will be modified as follows:

$$h(t) = \alpha(t)\, w(t) = A_g \cos(2\pi f_g t + \theta_g)\, w(t)$$

where $w(t)$ is the weighting function. The DFT of $h(t)$ is defined as

$$\bar{H}_k = \frac{1}{N} \sum_{n=0}^{N-1} h(nT_s)\, e^{-i2\pi kn/N}$$

$$= |\bar{H}_k|\, e^{i\phi_k} \quad k = 0, \ldots, N-1; \; n = 0, \ldots, N-1$$

where T_s is the sampling interval.

If f_r denotes the frequency of the dominant frequency line (i.e., closest to the true frequency f_g), and β the frequency bin spacing ($\beta = 1/(NT_s)$), the interpolation fraction v is defined by

$$v = \frac{f_g - f_r}{\beta} \qquad -\frac{1}{2} \le v < \frac{1}{2}$$

The amplitude ratio is defined by

$$R = \frac{|\bar{H}_r|}{|\bar{H}_{r\pm 1}|}$$

where the positive sign is used when $|\bar{H}_{r+1}| \ge |\bar{H}_{r-1}|$, and the negative sign when $|\bar{H}_{r-1}| > |\bar{H}_{r+1}|$.

Assume first the rectangular window $w(t) \equiv 1$; then

$$v \sim \pm \frac{1}{1+R} \tag{A2}$$

$$A_g \sim N \frac{2 \sin(\pi v/N)}{\sin(\pi v)} |\bar{H}_r|$$

and

$$\theta_g \sim \phi_r - \frac{\pi(N-1)}{N} v \tag{A3}$$

Thus equations (A2) and (A3) give the A_g and θ_g required in equation (A1).

Consider now the Hanning window given by

$$w(nT_s) = \frac{A_h}{2}\left(1 - \cos\frac{2\pi n}{N}\right) \qquad n = 0, \ldots, N-1$$

where $A_h = \sqrt{8/3}$ is used to normalize the mean square value of the window. Then

$$v \sim \pm \frac{2-R}{1+R}$$

$$A_g \sim N \frac{2(1-v^2)\sin(2\pi v/N)}{A_h \sin(\pi v)} |\bar{H}_r| \tag{A4}$$

and

$$\theta_g \sim \phi_r - \pi v \tag{A5}$$

where in the expression for A_g the approximation

$$v \sim \frac{\tan(\pi v/N)}{\tan(\pi/N)}$$

was made. Equations (A4) and (A5) give the parameters required in equation (A1).

References

1. Nieberding, W. C.; and Pollack, J. L.: Optical Detection of Blade Flutter in YF-100 Turbofan Engine. ASME Paper 77-GT-66, 1977.
2. Kurkov, A.; and Dicus, J.: Synthesis of Blade Flutter Vibratory Patterns Using Stationary Transducers. ASME Paper 78-GT-160, 1978.
3. Kurkov, A. P.: Flutter Spectral Measurements Using Stationary Pressure Transducers. J. Eng. Power, vol. 103, no. 2, Apr. 1981, pp. 461-467.
4. Kurkov, A. P.: Measurement of Aerodynamic Work During Fan Flutter. J. Eng. Power, vol. 105, no. 1, Jan. 1983, pp. 204-211.
5. Kurkov, A. P.: Measurement of Self-Excited Rotor-Blade Vibrations Using Optical Displacements. ASME Paper 83-GT-132, 1983.
6. Whitehead, D. S.: Torsional Flutter of Unstalled Cascade Blades at Zero Deflection. R&M-3429, British A.R.C., 1966.
7. Stearns, Samuel D.: Digital Signal Analysis. Hayden Book Co., 1975.
8. Singleton, Richard C.: An Algorithm for Computing the Mixed Radix Fast Fourier Transform. IEEE Trans. Audio and Electroacoust., vol. AU-17, no. 2, June 1969, pp. 93-103.

1. Report No.	2. Government Accession No.	3. Recipient's Catalog No.
NASA TP-2296		

4. Title and Subtitle	5. Report Date
Formulation of Blade-Flutter Spectral Analyses in Stationary Reference Frame	March 1984
	6. Performing Organization Code: 505-40-5A
7. Author(s): Anatole P. Kurkov	8. Performing Organization Report No.: E-1888
	10. Work Unit No.
9. Performing Organization Name and Address: National Aeronautics and Space Administration, Lewis Research Center, Cleveland, Ohio 44135	11. Contract or Grant No.
	13. Type of Report and Period Covered: Technical Paper
12. Sponsoring Agency Name and Address: National Aeronautics and Space Administration, Washington, D.C. 20546	14. Sponsoring Agency Code

15. Supplementary Notes

16. Abstract

Analytic representations are developed for the discrete blade deflection and the continuous tip static pressure fields in a stationary reference frame. Considered are the sampling rates equal to the rotational frequency, equal to the blade passing frequency, and for the pressure, equal to a multiple of the blade passing frequency. For the last two rates the expressions for determining the nodal diameters from the spectra are included. A procedure is presented for transforming the complete unsteady pressure field into a rotating frame of reference. The determination of the true flutter frequency by using two sensors is described. To illustrate their use, the developed procedures are used to interpret selected experimental results.

17. Key Words (Suggested by Author(s))	18. Distribution Statement
Flutter Aeroelasticity Blade vibration	Unclassified - unlimited STAR Category 07

19. Security Classif. (of this report)	20. Security Classif. (of this page)	21. No. of pages	22. Price*
Unclassified	Unclassified	31	A03

*For sale by the National Technical Information Service, Springfield, Virginia 22161

NASA-Langley, 1984

1 1 1U,A, 840321 S00903DS
DEPT OF THE AIR FORCE
AF WEAPONS LABORATORY
ATTN: TECHNICAL LIBRARY (SUL)
KIRTLAND AFB NM 87116